






## Article

# Genome Study of $\alpha$ -, $\beta$ -, and $\gamma$ -Carbonic Anhydrases from the Thermophilic Microbiome of Marine Hydrothermal Vent Ecosystems

Mohammad Sadegh Gheibzadeh <sup>1</sup>, Colleen Varaidzo Manyumwa <sup>2</sup>, Özlem Tastan Bishop <sup>2</sup>, Hossein Shahbani Zahiri <sup>1</sup>, Seppo Parkkila <sup>3,4</sup> and Reza Zolfaghari Emameh <sup>1,\*</sup>

<sup>1</sup> Department of Energy and Environmental Biotechnology, National Institute of Genetic Engineering and Biotechnology (NIGEB), Tehran 14965/161, Iran; m\_gheibzadeh@nigeb.ac.ir (M.S.G.); shahbani@nigeb.ac.ir (H.S.Z.)

<sup>2</sup> Research Unit in Bioinformatics (Rubi), Department of Biochemistry and Microbiology, Rhodes University, Grahamstown 6140, South Africa; colleen.manyumwa06@gmail.com (C.V.M.); o.tastanbishop@ru.ac.za (Ö.T.B.)

<sup>3</sup> Faculty of Medicine and Health Technology, Tampere University, 33520 Tampere, Finland; seppo.parkkila@tuni.fi

<sup>4</sup> Fimlab Ltd., Tampere University Hospital, 33520 Tampere, Finland

\* Correspondence: zolfaghari@nigeb.ac.ir; Tel.: +98-21-44787476

**Simple Summary:** Hydrothermal vents are regions such as hot springs found on the seafloor in the mid-ocean and near tectonic plates. They contain fluids with highly enriched carbon dioxide, which is the central element of life on Earth. Many organisms live in this environment and can survive in extreme conditions (extremophiles), such as up to 400 °C or higher, low pH, and high pressure. All organisms need the carbonic anhydrase (CA) enzyme to handle the acid-base imbalance through the hydration of carbon dioxide and the production of bicarbonate necessary for pH homeostasis and many cellular functions. The CAs have been categorized into eight families. In this study, we focused on  $\alpha$ -,  $\beta$ -, and  $\gamma$ -CAs from the thermophilic microbiome of marine hydrothermal vents. Microorganisms in this environment need CA to capture CO<sub>2</sub>, which is an important contribution to marine hydrothermal vent ecosystem functioning. Previously, we showed the transfer of  $\beta$ -CA gene sequences from prokaryotes to protozoans, insects, and nematodes via horizontal gene transfer (HGT). HGT is not only the transfer and movement of genetic information between organisms but is also a powerful tool in natural biodiversity. If the CA coding gene is transferred horizontally between microorganisms in hydrothermal vents, it is hypothesized that CA is essential for survival in these environments and one of the key players in the carbon cycle in the ocean.



**Citation:** Gheibzadeh, M.S.; Manyumwa, C.V.; Tastan Bishop, Ö.; Shahbani Zahiri, H.; Parkkila, S.; Zolfaghari Emameh, R. Genome Study of  $\alpha$ -,  $\beta$ -, and  $\gamma$ -Carbonic Anhydrases from the Thermophilic Microbiome of Marine Hydrothermal Vent Ecosystems. *Biology* **2023**, *12*, 770. <https://doi.org/10.3390/biology12060770>

Academic Editors: Daniel Puppe, Panayiotis Dimitrakopoulos and Baorong Lu

Received: 23 March 2023

Revised: 17 May 2023

Accepted: 17 May 2023

Published: 25 May 2023



**Copyright:** © 2023 by the authors. Licensee MDPI, Basel, Switzerland. This article is an open access article distributed under the terms and conditions of the Creative Commons Attribution (CC BY) license (<https://creativecommons.org/licenses/by/4.0/>).

**Abstract:** Carbonic anhydrases (CAs) are metalloenzymes that can help organisms survive in hydrothermal vents by hydrating carbon dioxide (CO<sub>2</sub>). In this study, we focus on alpha ( $\alpha$ ), beta ( $\beta$ ), and gamma ( $\gamma$ ) CAs, which are present in the thermophilic microbiome of marine hydrothermal vents. The coding genes of these enzymes can be transferred between hydrothermal-vent organisms via horizontal gene transfer (HGT), which is an important tool in natural biodiversity. We performed big data mining and bioinformatics studies on  $\alpha$ -,  $\beta$ -, and  $\gamma$ -CA coding genes from the thermophilic microbiome of marine hydrothermal vents. The results showed a reasonable association between thermostable  $\alpha$ -,  $\beta$ -, and  $\gamma$ -CAs in the microbial population of the hydrothermal vents. This relationship could be due to HGT. We found evidence of HGT of  $\alpha$ - and  $\beta$ -CAs between *Cycloclasticus* sp., a symbiont of *Bathymodiolus heckeriae*, and an endosymbiont of *Riftia pachyptila* via Integrins. Conversely, HGT of  $\beta$ -CA genes from the endosymbiont *Tevnia jericchonana* to the endosymbiont *Riftia pachyptila* was detected. In addition, *Hydrogenovibrio crunogenus* SP-41 contains a  $\beta$ -CA gene on genomic islands (GIs). This gene can be transferred by HGT to *Hydrogenovibrio* sp. MA2-6, a methanotrophic endosymbiont of *Bathymodiolus azoricus*, and a methanotrophic endosymbiont of *Bathymodiolus puteoserpentis*. The endosymbiont of *R. pachyptila* has a  $\gamma$ -CA gene in the genome. If  $\alpha$ - and  $\beta$ -CA coding genes have been derived from other microorganisms, such as endosymbionts of

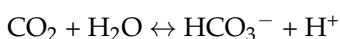
*T. jerichonana* and *Cycloclasticus* sp. as the endosymbiont of *B. heckeriae*, through HGT, the theory of the necessity of thermostable CA enzymes for survival in the extreme ecosystem of hydrothermal vents is suggested and helps the conservation of microbiome natural diversity in hydrothermal vents. These harsh ecosystems, with their integral players, such as HGT and endosymbionts, significantly impact the enrichment of life on Earth and the carbon cycle in the ocean.

**Keywords:** big data mining; carbonic anhydrase; extreme ecosystems; horizontal gene transfer; hydrothermal vents; mobile genetic elements; thermophilic microbiome

## 1. Introduction

Deep-sea hydrothermal vents are one of the best environments for evolutionary studies. Hydrothermal vents are regions such as hot springs found on the seafloor. These are located in the mid-ocean and near tectonic plates initially discovered in 1977 at a depth of 2.5 km around a hot spring on the Galápagos volcanic rift (spreading ridge) off the coast of Ecuador [1,2]. Based on their characteristics, deep-sea hydrothermal vents are called either black smokers or white smokers [3]. Black smokers' fluid temperature goes up to 400 °C or above and has a low pH, but white smokers have an alkaline pH, and their temperature is approximately 40–75 °C [3]. Hydrothermal vents contain fluids with highly enriched carbon dioxide (CO<sub>2</sub>), which are discharged into the deep sea by these vents [4]. CO<sub>2</sub> is a very stable form of carbon, the central element of life on Earth, and consists of a carbon atom covalently double-bonded to two oxygen atoms. Carbonic acid (H<sub>2</sub>CO<sub>3</sub>) is derived from the reaction of CO<sub>2</sub> and water molecules, so the product is an unstable compound that spontaneously splits into bicarbonate (HCO<sub>3</sub><sup>−</sup>) and protons (H<sup>+</sup>).

Many organisms live in this environment, especially bacterial and archaeal species that can survive in extreme conditions such as high temperatures and pressure. The organisms adapted to this habit are called extremophiles. All organisms need carbonic anhydrases (CAs) to handle the large amount of CO<sub>2</sub> and, consequently, the related acid-base imbalance [5–7]. CA is the metalloenzyme that catalyzes the reversible hydration of CO<sub>2</sub> to HCO<sub>3</sub> and H<sup>+</sup> as follows:



CAs are encoded by eight evolutionarily divergent gene families, including alpha (α), beta (β), gamma (γ), delta (δ), zeta (ζ), eta (η), theta (θ), and iota (ι) CA. α-CA has been reported in vertebrates, prokaryotes, fungi, algae, protozoa, and plants [7]. β-CA is expressed in prokaryotes, plants, fungi, protozoa, arthropods, and nematodes [8–13]. γ-CA is present in many plants, fungi, and prokaryotes. δ-CA and ζ-CA are present in marine diatoms [7,12]. η-CA was identified in the causative agent of malaria, *Plasmodium* spp., and θ-CA was identified in marine diatoms [7,14,15]. Iota(ι)-CA was recently reported to be expressed in diatoms and bacteria [16]. In this study, we focused on α-, β-, and γ-CAs from the thermophilic microbiome of marine hydrothermal vents. These metalloenzymes have an active site containing a Zn(II) metal ion cofactor [17], while Co(II) and Fe(II) can be included in α- and γ-CA, respectively [7]. The structures of α-CAs are frequently monomers and rarely dimers [18]; β-CAs are dimers, tetramers, or octamers [19]; and γ-CAs are trimers [20].

A previous study showed that β-CA gene sequences could be transferred from prokaryotes to protozoans, insects, and nematodes via HGT [21]. Additionally, the involvement of bacterial β-CA gene sequences in the gastrointestinal tract and their horizontal transfer to their host during evolution has been demonstrated [22]. HGT, also called lateral gene transfer (LGT), is the transfer and movement of genetic information between organisms and thus is differentiated from the vertical transmission of genes from parent to the next generations [23]. HGT plays a crucial role in natural biodiversity as a general mechanism [24,25],

and it often causes dramatic changes in the ecological and pathogenic properties of bacterial species, thereby promoting microbial diversification and speciation [25]. HGT may occur via mobile genetic elements (MGEs) such as integrons, genomic islands (GIs), integrative conjugative elements (ICEs), transposable elements (TEs), plasmids, and phages [26–30]. MGEs are parts of DNA that encode enzymes and other proteins that interpose the transfer of DNA in HGT within genomes (intracellular mobility) or between bacterial cells (intercellular mobility) [26]. Intercellular transfer of DNA takes three forms in prokaryotes: transformation, conjugation, and transduction [31].

Integrons are MGEs that allow the capture and expression of exogenous genes. Integrons have three essential core features: *intI*, *attI*, and *Pc* [32,33]. *intI* is the gene encoding an enzyme for catalyzing recombination between incoming gene cassettes called integron integrase (*IntI*) [32]. *AttI* is an integron-associated recombination site [33], and *Pc* is an integron-associated promoter that is expressed once a gene cassette is recombined [34]. The length of GIs is more than 10 kb, a part of a chromosome, recognized as discrete DNA segments, and can be different from closely related strains, and transposase is a primary tool for HGT through GIs [32–34]. Another family of MGEs is the integrative conjugative element (ICE), called the conjugative transposon. ICEs have two features: first, they are integrated into a host genome, and second, they encode a type IV secretion system (functional conjugation system) [28,35]. TEs are DNA sequences that can move from one location to another in the genome [30]. TEs fall into two classes: retrotransposons (Class I) or RNA transposons [36] and true transposons (Class II) or DNA transposons that consist of a transposase gene with two terminal inverted repeats (TIRs) on either side [30]. Additionally, insertion sequences (IS) are small MGEs that carry more than one or two transposase genes [37]. The CA genes may be transferred between organisms living in hydrothermal vents and their endosymbionts via HGT. Endosymbiotic bacteria are located in the trophosome of the host, which contains animal cells, so-called bacteriocytes [38]. For instance, one of the important living organisms living in deep-sea hydrothermal vents is the giant tubeworm *Riftia pachyptila*, which lives with its symbiont bacteria. Nitrate, oxygen, hydrogen sulfide, and inorganic carbon are taken up from the environment and it feeds its symbiotic bacteria with these substances in an organ known as the trophosome [39].

In addition, about one-third of the added carbon from atmospheric CO<sub>2</sub> uptake into the ocean increases dissolved CO<sub>2</sub> in seawater [40]. The accompanying acidification may reduce the seawater saturation of calcite, thus affecting marine calcifications. CA helps the concentration of inorganic carbon in the fluid from which calcium carbonate is sedimented and directly affects the calcification in some calcifiers, such as gastropods, oysters, and giant clams as well as coral calcification. The calcification can be reduced by 40%, which has been affected by high atmospheric CO<sub>2</sub> levels. Even a modest impact on producing carbonate shells and skeletons may have important consequences on the global carbon cycle [41].

Microorganisms in this environment need CA to capture CO<sub>2</sub>, which is an important contribution to marine hydrothermal vent ecosystem functioning [42]. It has been suggested that  $\alpha$ -CA evolution may contribute to the vulnerability to environmental changes of bivalves and their diversity [43] since HGT would create a large variability acted on by natural selection [39]. If the coding gene of this enzyme is transferred horizontally between hydrothermal vent microorganisms, it is hypothesized that CA is essential for survival and for preserving natural biodiversity in this extreme ecosystem. For this purpose, we investigated the evolutionary relationship and the possibility of HGT in the hydrothermal vent ecosystem. We conducted a large data mining and bioinformatics study focusing on the HGT of  $\alpha$ -,  $\beta$ - and  $\gamma$ -CA genes in the microbial population of deep-sea hydrothermal vents.

## 2. Materials and Methods

### 2.1. Identification of $\alpha$ -, $\beta$ -, and $\gamma$ -CA Sequences

We collected the names of all microbial populations from hydrothermal vents based on the literature. The protein and DNA sequences of CA candidates were retrieved from databases that were previously annotated in these databases after performing genomics

and proteomics studies (Tables S1–S3). We retrieved their  $\alpha$ -,  $\beta$ -, and  $\gamma$ -CA protein sequences from UniProt (<http://www.uniprot.org/>, 1 March 2023). In addition, we utilized a Position-Specific Iterated BLAST (PSI-BLAST) in the National Center for Biotechnology Information (NCBI) for two iterations to identify sequences that were homologous to the query sequences from organisms originating from hydrothermal vents. Each CA family has a defined conserved amino acid sequence to retrieve other CAs from the relevant CA family.  $\alpha$ -CAs have three conserved histidine residues [21] (Figure 1A) that can be used as a pattern for identifying bacterial  $\alpha$ -CAs.  $\beta$ -CAs have two highly conserved motifs; the first motif includes three residues of cysteine, aspartic acid, and arginine (Cx Dx R); the second highly conserved motif includes histidine and cysteine residues (HxxC) [21] (Figure 1B).  $\gamma$ -CAs have three histidine residues as well as asparagine and glutamine residues (Nx QxxxxH) and (HxxxxH) [44,45] (Figure 1C).

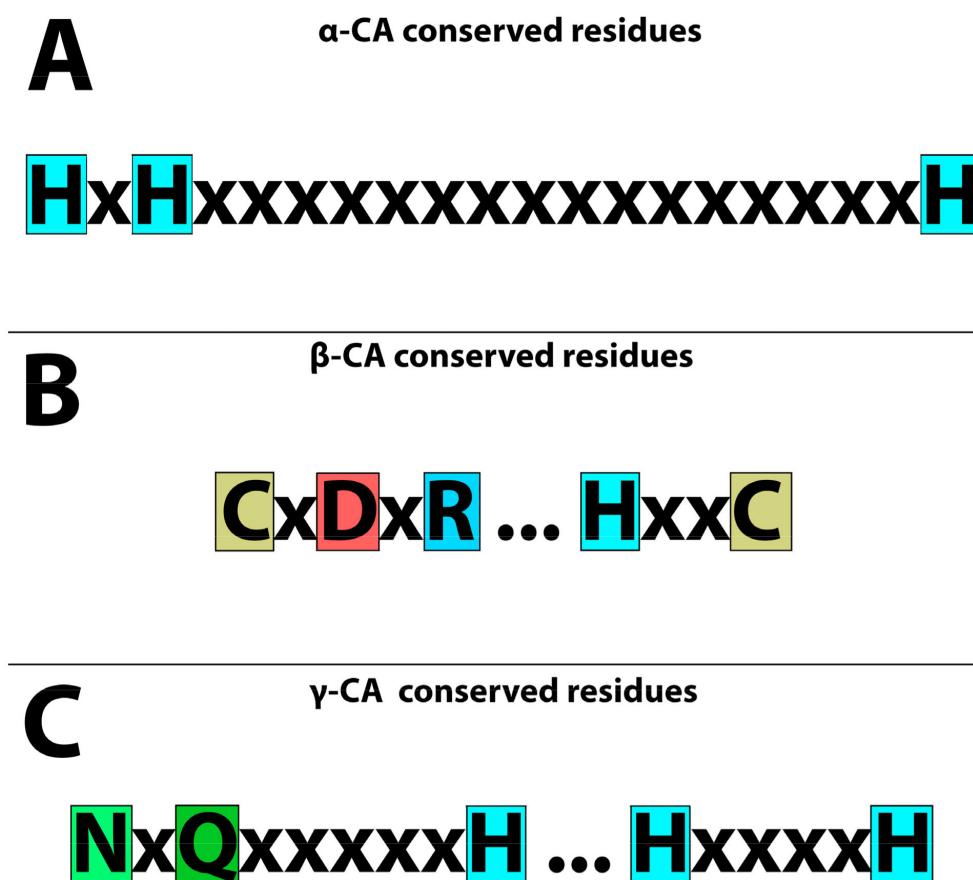


**Figure 1.** Conserved residues of CAs in the catalytic active sites. (A) Three “H” histidines are highly conserved in  $\alpha$ -CAs. (B) Two cysteines “C”, one histidine “H”, one aspartic acid “D”, and one arginine “R” are highly conserved amino acids in  $\beta$ -CAs. (C) Three histidine residues “H”, one asparagine “N”, and one glutamine “Q” are highly conserved amino acids in  $\gamma$ -CAs.

In addition,  $\alpha$ -,  $\beta$ -, and  $\gamma$ -CA proteins from the microbiome of marine hydrothermal vent ecosystems with taxonomic classifications have been listed in Table S1 [46–62], Table S2 [63–95], and Table S3 [96–118], respectively.

Multiple sequence alignment (MSA) was performed using the Tree-based Consistency Objective Function for Alignment Evaluation (T-Coffee) [119] for the identification of conserved residues in  $\alpha$ -,  $\beta$ -, and  $\gamma$ -CA protein sequences. Additionally, we analyzed these MSA results in Jalview2 software [120]. Then, we made a dataset for each organism (the whole genome, if available) from the NCBI database (<https://www.ncbi.nlm.nih.gov/nuccore>) (Access date: 1 March 2023) and apperceived the  $\alpha$ -,  $\beta$ -, and  $\gamma$ -CA gene positions on our bacterial genomes from the Ensembl Bacteria (<https://bacteria.ensembl.org>) (Access

date: 1 March 2023) and KEGG (<https://www.genome.jp/kegg/>) (Access date: 1 March 2023) databases. We annotated our integrons via Geneious prime version: 2021.0.3 software with default parameters.

## 2.2. Phylogenetic Analysis

We retrieved the Tax ID of all microbiomes from marine hydrothermal vents containing  $\alpha$ -,  $\beta$ -, and  $\gamma$ -CA from the UniProt database (<https://www.uniprot.org/taxonomy/>) (Access date: 1 March 2023) and NCBI database (<https://www.ncbi.nlm.nih.gov/taxonomy/>) (Access date: 1 March 2023) for more accuracy. Phylogenetic trees were constructed for evolutionary study using maximum likelihood, and models with the lowest Bayesian Information Criterion (BIC) scores were considered to best describe the substitution pattern [121] via MEGA X software [122] and annotated in FigTree V1.4.4 software for all protein sequences. Then, we generated a heatmap based on the pairwise sequence identity between them using GraphPad Prism version 8.00 software for Windows ([www.graphpad.com](http://www.graphpad.com), 1 March 2023).

## 2.3. Identification of $\alpha$ -, $\beta$ -, and $\gamma$ -CA Genes on the MGEs

### 2.3.1. Integrons

Integrons have three essential core features: *intI*, *attI*, and *Pc* [32–34], so we tried to find these features in our dataset. Integrons gain new genes as part of gene cassettes [123]. In addition to these features, we needed to find cassettes as simple structures consisting of a single open reading frame (ORF) bounded by a cassette-associated recombination site called a 59-base element or *attC* [124]. Gene cassettes exist in a circular free state and are integrated into *attI* [125,126]. Integron integrase mediates the integration of circular gene cassettes by site-specific recombination between *attI* and *attC* reversibly and excises [126–128]. For the identification of the mentioned features, we used the Integron finder. Integron Finder has two forms: a standalone program ([https://github.com/gem-Pasteur/Integron\\_Finder](https://github.com/gem-Pasteur/Integron_Finder)) (Access date: 1 March 2023) and a web application (<https://galaxy.pasteur.fr/#forms::integronfinder>) (Access date: 1 March 2023). Hidden Markov model (HMM) profiles were used for the search of integron-integrase and covariance models for *attC* sites. Pattern matching was also used for other features (such as promoters and *attI* sites) [129]. In this study, we applied the web application of integron finder.

### 2.3.2. Genomic Islands (GIs)

Prediction of GIs was studied using tools such as SIGI-HMM, IslandPath-DIMOB [130], PAI-IDA [131], and Centroid [132], based on the evaluation of sequence compositions as well as BLAST homology searches and whole-genome sequence alignment for comparative genomics methods [48]. For this purpose, we applied the IslandViewer 4 (<http://www.pathogenomics.sfu.ca/islandviewer/>) (Access date: 1 March 2023) database using a web server to predict and visualize genomic islands in bacterial and archaeal genomes [133]. After searching all microorganisms in this database, we retrieved their annotations and searched for  $\alpha$ -,  $\beta$ -, and  $\gamma$ -CA genes on their GIs.

### 2.3.3. Integrative Conjugative Elements (ICEs)

ICEs comprise the ICE integration and excision module, ICE conjugation module, and ICE regulation module, which are the main genetic modules [134]. ICEs contain integrase- and relaxase-coding genes and/or type IV secretion systems. For the identification of ICEs, we used ICEberg 2.0 (<https://db-mml.sjtu.edu.cn/ICEberg/>) (Access date: 1 March 2023) [135,136].

### 2.3.4. Transposable Elements (TEs), Phages, and Plasmids

Insertion sequences (IS) and true transposons (Tn) consist of a transposase gene with two terminal inverted repeats (TIRs) on either side [30]. IS are small mobile elements that carry little more than one or two transposase genes [37]. For the identification of

these elements, we used the MobileElementFinder web server (<https://cge.cbs.dtu.dk/services/MobileElementFinder/>) (Access date: 1 March 2023) [137]. To study phages in our datasets, we needed to find evidence of prophages. Evidence of insertion sites includes alteration of GC content and the presence of tRNA flanking the region [138]. PhageWeb (<http://computationalbiology.ufpa.br/phageweb/>) (Access date: 1 March 2023) was used to search for this evidence. Utilizing information from a 2018 study by Sousa, A.L.d., et al., we set options to default (BLAST options to identify 80% and six minimum of CDS) in prophage identification [139]. After that, we checked the location of our genes for the position on the chromosome or plasmid.

### 3. Results

#### 3.1. Identification of $\alpha$ -, $\beta$ -, and $\gamma$ -CA and Protein Sequences

This study evaluated 83 previously isolated microorganisms in or around hydrothermal vents (Tables S1–S3). They consisted of bacteria and archaea and were classified into ten groups of bacterial species, including Alphaproteobacteria, Deltaproteobacteria, Epsilonproteobacteria, Gammaproteobacteria, Zetaproteobacteria, Aquificae, Bacilli, Deferribacteres, Deinococci, and Fusobacteria, as well as four groups for archaea, including Archaeoglobi, Methanopyri, Methanococci, and Thermococci. We retrieved 25  $\alpha$ -CA, 55  $\beta$ -CA, and 47  $\gamma$ -CA protein sequences from the UniProt database [140]. We must note that we have abbreviated microorganism names for convenience, and they are stated in the Supplementary Materials (Tables S1–S3). It is worth noting that many of these isolated species from hydrothermal vents are endosymbiotic microorganisms.

The results of the MSA for verification of  $\alpha$ -,  $\beta$ -, and  $\gamma$ -CA protein sequences are shown in the Supplementary Materials (Figures S1–S3). Many  $\alpha$ -CAs from the thermophilic microbiome of marine hydrothermal vents have been studied previously [42]. At first, the MSA of  $\alpha$ -CA showed conserved residues (Figure S1) in which three conserved histidine residues (His107, His109, and His126) [21] were visible and coordinated with the Zn<sup>2+</sup> metal ion cofactor in the enzyme catalytic active site [141]. Next, the MSA of  $\beta$ -CAs showed three conserved residues in the first highly conserved motif (Cx DxR), including cysteine, aspartic acid, and arginine, with variation in the residues between them [21]. The second highly conserved motif (HxxC), which contained histidine and cysteine residues with two other residues between them, was also observed [21] (Figure S2). Finally, in the MSA of  $\gamma$ -CAs, we identified three histidine residues, asparagine and glutamine residues, that were highly conserved [44,45] (Figure S3).

#### 3.2. Phylogenetic Analysis

The results of phylogenetic analysis and heatmaps of  $\alpha$ -,  $\beta$ -, and  $\gamma$ -CAs from the thermophilic microbiome of hydrothermal vents are shown in Figure 2, Figure 3, and Figure 4, respectively. We highlighted the bacterial CAs with blue and archaea with orange. The evolutionary history was inferred using the maximum-likelihood method and the result of calculating the best model using the Le Gascuel model with discrete gamma distribution and invariable sites (LGGI) [142]. Since the phylogenetic analysis of  $\alpha$ -CAs from the thermophilic microbiome of marine hydrothermal vents has been studied previously [42], we analyzed additional species, including *Hydrogenovibrio crunogenus* (XCL-2), *Hydrogenovibrio crunogenus* (SP-41), *Bacillus oceanisediminis*, *Sulfurovira caldicuralii*, *Caldithrix abyssi*, an endosymbiont of *Riftia pachyptila* (vent Ph05), *Bathymodiolus platifrons* as a methanotrophic gill symbiont, and *Cycloclasticus* sp. as symbionts of *Bathymodiolus heckerae*, *Nitrosophilus alvini*, *Nitrosophilus labii*, *Sulfurimonas paralvinellae*, *Hydrogenimonas urashimensis*, *Sulfurovum indicum* and *Persephonella atlantica* (Figure 2).

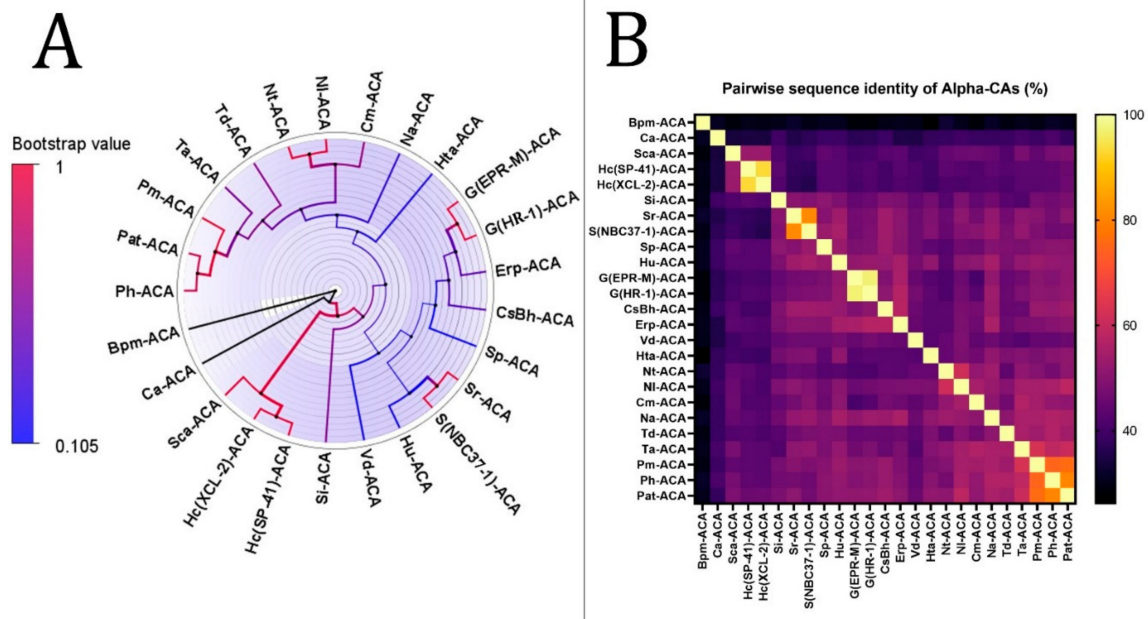


**Figure 2.** Phylogenetic analysis of  $\alpha$ -CAs from the thermophilic microbiome of hydrothermal vents. (A) The tree’s branches and nodes were colored based on bootstrap values (0–1), and the bacterial CAs and archaea were highlighted with blue and orange, respectively, via FigTree V1.4.4 software. (B)  $\alpha$ -CA pairwise sequence identity heatmap. The heatmap for the all-versus-all pairwise sequence identity of  $\alpha$ -CA calculations was generated using T-Coffee MSA. Pairwise sequence identity values are colored from yellow (highest) to black (lowest).

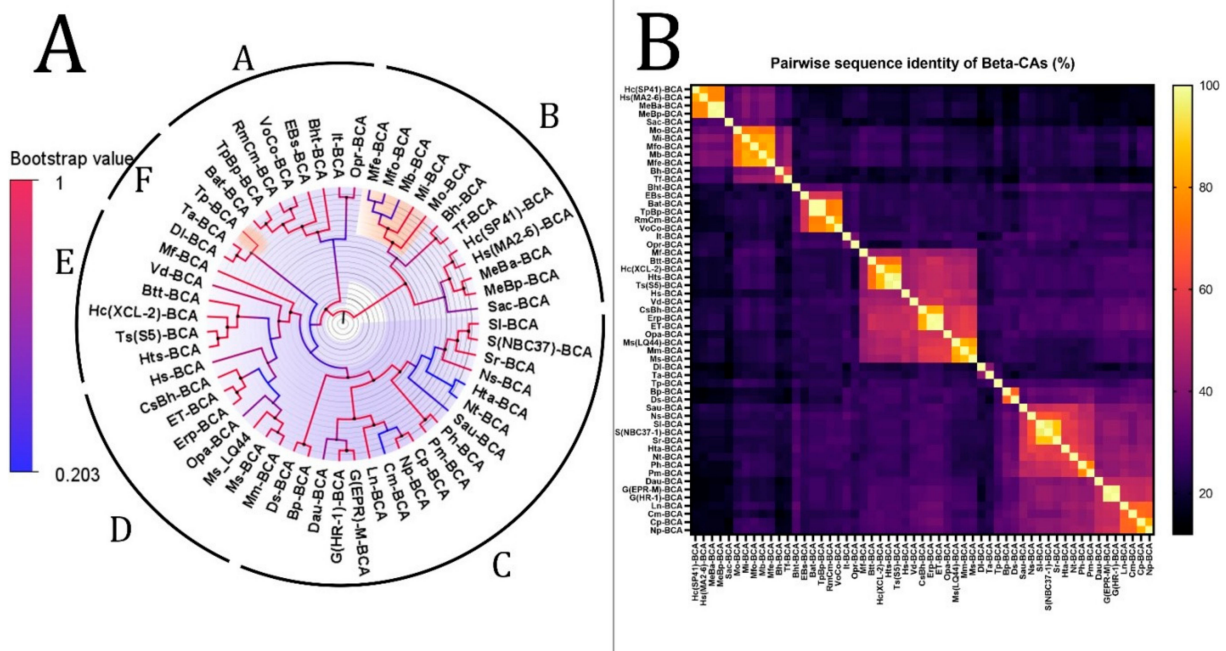


**Figure 3.** Phylogenetic analysis of  $\beta$ -CAs from the thermophilic microbiome of hydrothermal vents. (A) The tree’s branches and nodes were colored based on bootstrap values (0–1), and the bacterial CAs and archaea were highlighted with blue and orange via FigTree V1.4.4 software. (B)  $\beta$ -CA pairwise sequence identity heatmap. The heatmap for the all-versus-all pairwise sequence identity of  $\beta$ -CA calculations was generated using T-Coffee MSA. Pairwise sequence identity values are colored from yellow (highest) to black (lowest).

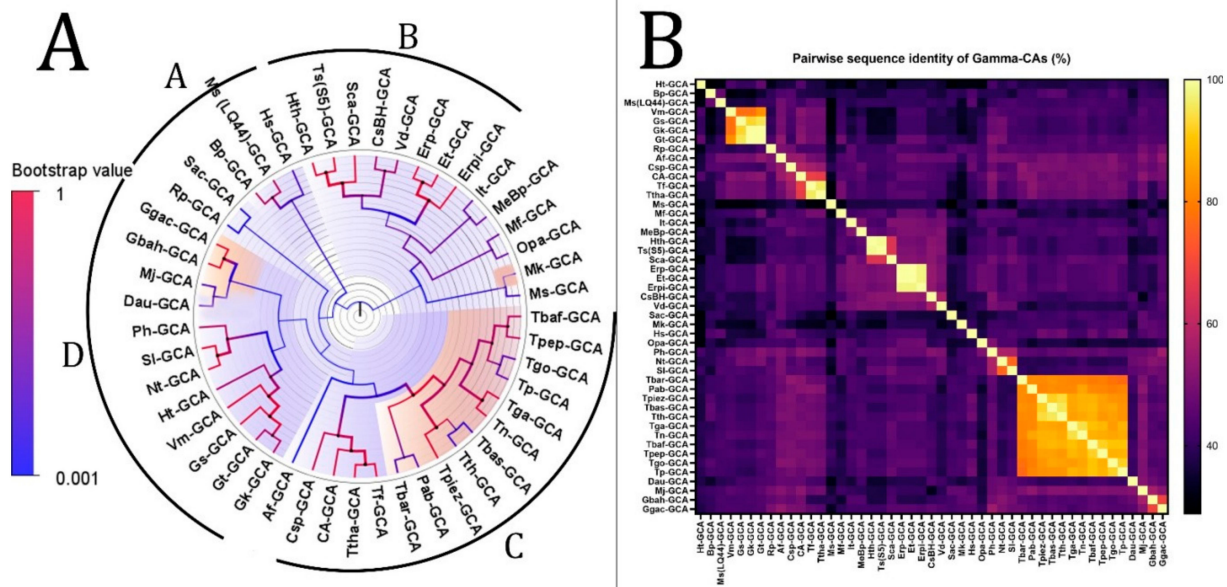


**Figure 4.** Phylogenetic analysis of  $\gamma$ -CAs from the thermophilic microbiome of hydrothermal vents. (A) The tree's branches and nodes were colored based on bootstrap values (0–1), and the bacterial CAs and archaea were highlighted with blue and orange, respectively, via FigTree V1.4.4 software. We did not find any specific items between clades A and B or between clades C and D that can be categorized as separate clades. (B)  $\gamma$ -CA pairwise sequence identity heatmap. The heatmap for the all-versus-all pairwise sequence identity of  $\gamma$ -CA calculations was generated using T-Coffee MSA. Pairwise sequence identity values are colored from yellow (highest) to black (lowest).

The phylogenetic tree of  $\alpha$ -CAs was performed with the highest log-likelihood (−9636.17). Initial trees for the heuristic search were obtained automatically by applying neighbor-joining and BioNJ algorithms to a matrix of pairwise distances estimated using the Jones-Taylor-Thornton (JTT) model and then selecting the topology with a superior log-likelihood value. A discrete gamma distribution was used to model evolutionary rate differences among sites (two categories (+G, parameter = 1.1935)). The rate variation model allowed some sites to evolve invariantly ([+I], 3.92% sites). The tree was drawn to scale, with branch lengths measured in the number of substitutions per site. Twenty-five  $\alpha$ -CA amino acid sequences were involved in this analysis. There were a total of 357 positions in the final dataset. The analysis revealed that there is a common ancestor between Hc(XCL-2)-ACA and Hc(SP-41)-ACA; Sr-ACA and S(NBC37-1)-ACA; G(EPR-M)-ACA and G(HR-1)-ACA; Nt-ACA and Nl-ACA; and Pat-ACA and Ph-ACA.

The phylogenetic tree of  $\beta$ -CAs with the highest log-likelihood (−15,146.85) is shown in Figure 3. Initial trees for the heuristic search were obtained automatically by applying neighbor-joining and BioNJ algorithms to a matrix of pairwise distances estimated using the JTT model and then selecting the topology with a superior log-likelihood value. A discrete gamma distribution was used to model evolutionary rate differences among sites (two categories (+G, parameter = 2.7462)). The rate variation model allowed some sites to evolve invariantly ([+I], 0.97% sites). This analysis involved 55  $\beta$ -CA amino acid sequences. There were a total of 308 positions in the final dataset. Based on bootstrap values and identity, we divided this tree (Figure 3) into six clades from A to F. The analysis revealed that there is a common ancestor between the  $\beta$ -CAs in each clade.

The phylogenetic tree of  $\gamma$ -CAs with the highest log-likelihood (−9786.77) is shown in Figure 4. The initial phylogenetic trees for the heuristic search were automatically obtained by applying Neighbor-Join and BioNJ algorithms to a matrix of pairwise distances estimated using the JTT model. The topology with a superior log-likelihood value was then



selected. A discrete gamma distribution was used to model evolutionary rate differences among sites (two categories (+G, parameter = 1.6179)). The variation model rate allowed some sites to evolve invariably ([+I], 3.65% sites). Forty-seven amino acid sequences were involved in this analysis. There were a total of 219 positions in the final dataset. We divided this tree into four clades from A to D based on bootstrap values and identity, similar to the  $\beta$ -CA phylogenetic analysis. The analysis revealed that there is a common ancestor between the  $\gamma$ -CAs in each clade.

### 3.3. Identification of $\alpha$ -, $\beta$ -, and $\gamma$ -CA Genes on MGEs

#### 3.3.1. Integrons

Integrons are divided into complete integrons, In0 elements, and CALINs elements. Complete integrons have an integrase and one *attC* site or more. The In0 elements consist of an integrase without *attC* sites, and CALINs have two *attC* sites or more without integrase. After searching integrase features on our dataset, we found integrons in many microorganisms, which have been mentioned in Table 1. We performed a BLAST analysis on all protein CDS (protein-coding sequences) on integrons. The results showed that only the endosymbiont of *R. pachyptila* and the endosymbiont of *Tevnia jerichonana* have CA-coding genes in their integrase area.

**Table 1.** Integrons in the thermophilic microbiome from hydrothermal vents.

Microorganisms	Integron Type	Integrase	CA Gene
<i>Cycloclasticus</i> sp. symbiont of <i>Bathymodiolus heckeriae</i>	In0	Intersection tyr intl	-
Endosymbiont of <i>Riftia pachyptila</i> (vent Ph05)	Integron 1: CALIN	-	$\alpha$ -CA
<i>Sulfurovum</i> sp. NBC37-1	Integron 2: CALIN	-	$\beta$ -CA
<i>Caldithrix abyssi</i>	CALIN	-	-
<i>Hydrogenovibrio crunogenus</i> SP-41	Integron 1: CALIN Integron 2: CALIN Integron 3: Complete Integron 4: CALIN	Intersection tyr intl	-
<i>Thiomicrospira crunogena</i> XCL-2	Integron 1: CALIN	-	-
<i>Bathymodiolus thermophilus</i>	Integron 2: CALIN	-	-
thioautotrophic gill symbiont	Integron 1: CALIN	-	-
Endosymbiont of	Integron 2: CALIN	-	-
<i>Tevnia jerichonana</i>	Integron 3: CALIN	-	-
<i>Halomonas sulfidaeris</i> strain SST4	CALIN CALIN	- -	$\beta$ -CA -
<i>Marinobacter</i> sp. LQ44	Integron 1: CALIN Integron 2: In0	Intersection tyr intl	-
<i>Sulfurimonas autotrophica</i>	Integron 1: In0 Integron 2: CALIN	Intersection tyr intl	-
Endosymbiont of <i>Bathymodiolus septemdiarum</i>	Integron 1: CALIN Integron 2: CALIN Integron 3: In0 Integron 4: CALIN Integron 5: CALIN	Intersection tyr intl	-
<i>Hydrogenovibrio thermophilus</i>	Complete	Intersection tyr intl	-
<i>Thermococcus barophilus</i> strain CH5	CALIN	-	-
<i>Cycloclasticus</i> sp. symbiont of <i>Bathymodiolus heckeriae</i>	In0	Intersection tyr intl	-
Endosymbiont of <i>Riftia pachyptila</i> (vent Ph05)	Integron 1: CALIN Integron 2: CALIN	-	$\alpha$ -CA $\beta$ -CA

Table 1. Cont.

Microorganisms	Integron Type	Integrase	CA Gene
<i>Sulfurovum</i> sp. NBC37-1	Integron 1: CALIN Integron 2: CALIN	-	-
<i>Caldithrix abyssi</i>	CALIN	-	-
<i>Hydrogenovibrio crunogenus</i> SP-41	Integron 1: CALIN Integron 2: CALIN Integron 3: Complete Integron 4: CALIN	Intersection tyr intl	-
<i>Thiomicrospira crunogena</i> XCL-2	Integron 1: CALIN Integron 2: CALIN	-	-
<i>Bathymodiolus thermophilus</i> thioautotrophic gill symbiont	Integron 1: CALIN Integron 2: CALIN Integron 3: CALIN	-	-
Endosymbiont of <i>Tevnia jerichonana</i>	CALIN	-	$\beta$ -CA
<i>Halomonas sulfidaeris</i> strain SST4	CALIN	-	-
<i>Marinobacter</i> sp. LQ44	Integron 1: CALIN Integron 2: In0	Intersection tyr intl	-
<i>Sulfurimonas autotrophica</i>	Integron 1: In0 Integron 2: CALIN	Intersection tyr intl	-
Endosymbiont of <i>Bathymodiolus septemdiarium</i>	Integron 1: CALIN Integron 2: CALIN Integron 3: In0 Integron 4: CALIN Integron 5: CALIN	Intersection tyr intl	-
<i>Hydrogenovibrio thermophilus</i>	Complete	Intersection tyr intl	-
<i>Thermococcus barophilus</i> strain CH5	CALIN	-	-

According to data analysis by Integron Finder, the endosymbiont of *Riftia pachyptila* contains two integrons. The first integron has one CDS, and the second has two *attC* sites; the CALIN type has six CDSs, an  $\alpha$ -CA gene on the fourth CDS, and a  $\beta$ -CA gene on the sixth CDS (Figure 5A). The endosymbiont of *Tevnia jerichonana* has one integron with two *attC* sites, six CDS is CALIN type, and a  $\beta$ -CA gene on the fourth CDS (Figure 5B).

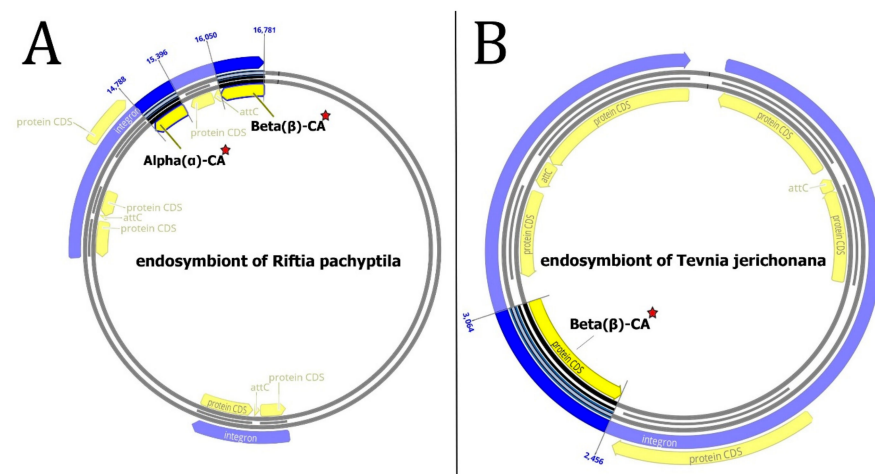
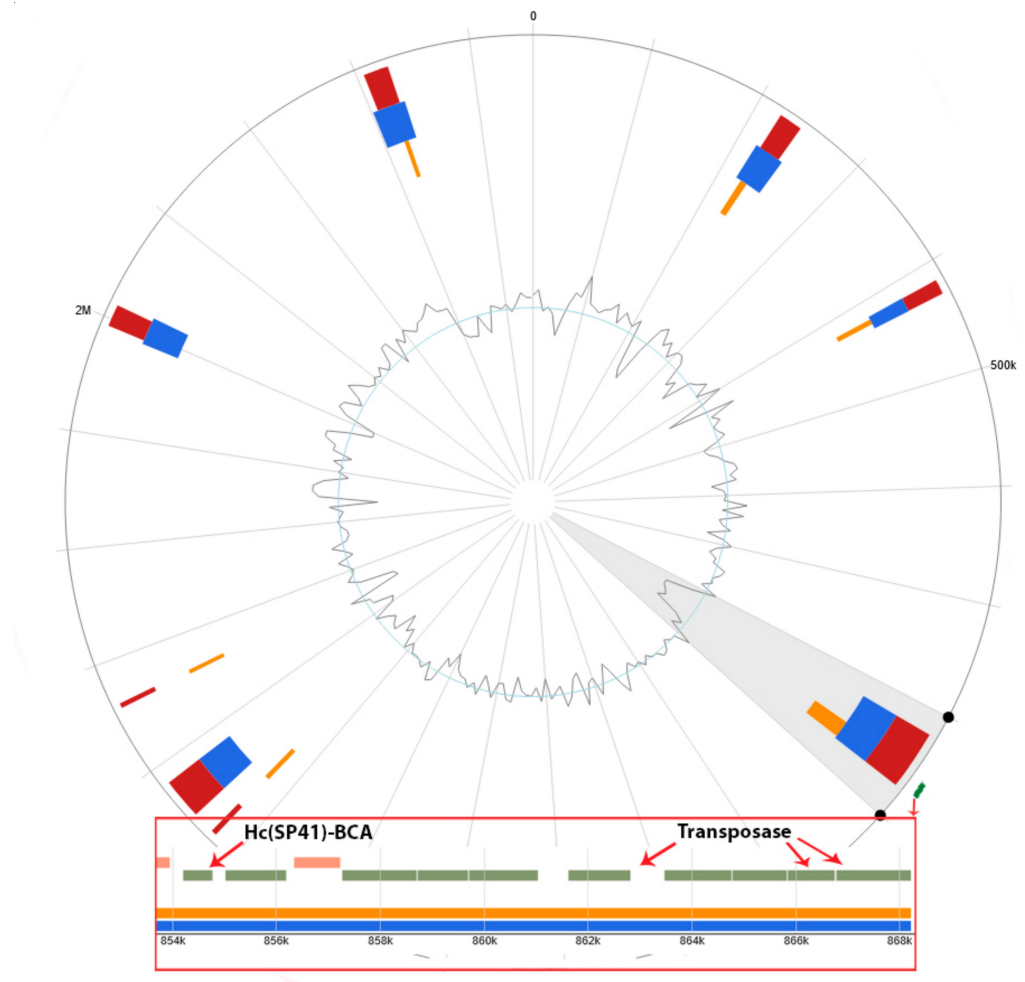


Figure 5. Integrons of endosymbionts of (A) *Riftia pachyptila* and (B) *Tevnia jerichonana*. The  $\alpha$ - and  $\beta$ -CA genes are bolded and marked with red stars.

### 3.3.2. Genomic Islands (GIs)

According to the IslandViewer 4 (<http://www.pathogenomics.sfu.ca/islandviewer/>) (Access date: 1 March 2023) database, 25 out of 83 of our microorganisms have GIs, and only one of the *Hydrogenovibrio crunogenus* SP-41 GIs carries a  $\beta$ -CA gene (*Hc(SP41)-BCA*) (UniProt ID: Q31FD6) and three transposase genes that are primary tools for HGT [143] (Figure 6). This GI is predicted by SIGI-HMM [144] and IslandPath-DIMOB methods [130]. However, the HGT of  $\beta$ -CA genes with GIs between prokaryotes and protists was previously studied [22].



**Figure 6.** GIs of *Hydrogenovibrio crunogenus* SP-41. *Hc(SP41)-BCA* and transposase genes are marked green and shown in the red box. The GC content is visible at the center of the figure.

### 3.3.3. Integrative Conjugative Elements (ICEs), Transposable Elements (TEs), Phages, and Plasmids

According to ICEberg 2.0 (<https://db-mml.sjtu.edu.cn/ICEberg/>) (Access date: 1 March 2023) and MobileElementFinder web server results, we did not find any  $\alpha$ -,  $\beta$ -, and  $\gamma$ -CA genes on the ICEs and TEs. Additionally, using PhageWeb (<https://github.com/phagewebufpa/API>) (Access date: 25 April 2019), we did not find any evidence supporting the transfer of  $\alpha$ -,  $\beta$ -, and  $\gamma$ -CA genes via phages. Based on the details of our dataset, CA genes were not located on the plasmids from the thermophilic microbiome of hydrothermal vents, and all genes were found on the chromosomes.

## 4. Discussion

The evolutionary process in hydrothermal vent ecosystems and the role of viruses in the biodiversity in this harsh environment have been studied previously. A study

performed by Cheng et al. [145] revealed that bacteriophages are the most predominant viruses across the global hydrothermal vents, while single-stranded DNA viruses, including Microviridae and small eukaryotic viruses, have been located in the next steps. The metagenomics analysis showed that this virome plays a crucial role in the evolution and biodiversity of the microbiome of hydrothermal vents, especially Gammaproteobacteria and Campylobacterota [145]. Although the bacteriophages have no role in the HGT of CA genes in the hydrothermal ecosystems, our previous studies showed the HGT of  $\beta$ -CA genes from prokaryotic endosymbionts to their protozoan, insects, and nematodes hosts. In addition, the genomic islands have been shown to have a potential role in the HGT of  $\beta$ -CA genes from ancestral prokaryotes to protists. Since then, no further study has been performed on the HGT of CA genes. Since hydrothermal vent ecosystems have been reported as potent environments for HGT and biodiversity, these harsh deep-sea fissures were studied.

According to the heatmap and phylogenetic analysis (Figure 2) of  $\alpha$ -CAs, Bpm-ACA and Ca-ACA showed no significant relationship with the other  $\alpha$ -CAs. Hc(XLC-2)ACA, Hc(SP41)-ACA, and Sca-ACA clustered together with branch bootstrap values of 1.00, showing significant relationships. Additionally, G(HR-1)-ACA and G(EPR-M)-ACA had a branch bootstrap value of 1.00, indicating a robust evolutionary relationship similar to that between Sr-ACA and S(NBC37-1)-ACA, whose bootstrap value was also 1.00. Similar to a previous study, the branch for Pm-ACA and Ph-ACA was observed to have a high bootstrap value of 0.99. A high branch bootstrap value of 0.86 was observed for CsBh-ACA and Erp-ACA. It is necessary to mention that all the  $\alpha$ -CAs above belong to the Proteobacteria phylum except for Pm-ACA and Ph-ACA, which belong to the Aquificae phylum. According to the heatmap and phylogenetic analysis (Figure 3) of  $\beta$ -CAs, in clade A, Opr-BCA and It-BCA have poor relationships with other clade members, showing a branch bootstrap value of 0.37. All members of clade B have the same root, but Mfe-BCA, Mfo-BCA, and Mb-BCA have poor relationships with other clade members. In clade C, a significant relationship between Sr-BCA, S(NBC37)-BCA, and Si-BCA showed a branch bootstrap value of 1.00, in which pairwise sequence identities of more than 88.6% were revealed. Although these three cases with a branch bootstrap value of 0.92 have a significant relationship with Ns-BCA, they have a poor relationship with other members of clade C. In clade D, a relationship between Erp-BCA, Et-BCA, and CsBh-BCA was observed with a 1.00 branch bootstrap value, in which a pairwise sequence identity of more than 83.5% was observed for all three. In clade E, the cluster containing Hts-BCA, Ts-BCA, Hc(XCL-2)-BCA, and Btt-BCA was observed with a branch bootstrap value of 1.00. Clade F with a 0.3 branch bootstrap value did not show a good relationship with other clades, while Di-BCA and Ta-BCA have the same root as Tp-BCA, a member of archaea. According to the heatmap and phylogenetic analysis of  $\gamma$ -CAs (Figure 4), clades A and B, with branch bootstrap values of 0.02 and 0.001, respectively, have a very poor relationship with other clades, including Erpi-GCA, Erp-GCA, and ET-GCA with different branch bootstrap values of more than 0.98 and a pairwise sequence identity value of more than 97.78, which have a significant relationship together. In addition, a meaningful relationship was observed for Hts-GCA, Ts(S5)-GCA, and Sca-GCA with a branch bootstrap value of 0.99. In clade C, archaea and bacteria have the same root, and according to the heatmap, all archaea have high pairwise sequence identity values. In clade D, Gbah-GCA and Ggac-GCA have a good relationship with a branch bootstrap value of 0.99 and a pairwise sequence identity value of 69.18. According to the heatmap of  $\gamma$ -CA (Figure 4B) in clade D, Gs-GCA with a branch bootstrap value of 0.99 and a pairwise sequence identity value of 94.29 had a significant relationship with Gk-GCA.

CALIN elements (Table 1) might have arisen from a missing integrase in a previously complete integron. The  $\alpha$ - and  $\beta$ -CA genes from CALIN may be cut by the integron-integrase and reinserted in the integron at an *attI* site. Since the stable circular form of CALINs can survive in the environment, these genetic elements can be taken up by transformable bacteria through a transformation mechanism [146]. On the other hand,

integrations often capture cassettes from CALIN elements [129], so the  $\alpha$ - and  $\beta$ -CA genes can be derived from different microorganisms or transferred to other hosts. According to the phylogenetic trees of  $\alpha$ - and  $\beta$ -CA (Figures 2A and 3A), Erp-ACA has the highest relationship with CsBh-ACA, with a bootstrap value of 0.40 and a pairwise sequence identity value of 57.61, which is a weak relationship. In addition, it has a relatively weak relationship with G(EPR-M)-ACA and G(HR-1)-ACA twins with a bootstrap value of 0.44 and pairwise sequence identity values of 55.19 and 57.39, respectively. The  $\beta$ -CAs in clades A and B, with 0.02 and 0.001 branch bootstrap values, respectively, did not have a good relationship with other clades. At the same time, Erp-BCA is the highest related compound to Et-BCA and CsBh-BCA, with a 1.00 branch bootstrap value and pairwise sequence identity of 99 and 100, respectively. Moreover, the  $\beta$ -CA gene (*Et-BCA*) from the endosymbiont of *T. jerichonana* is related the highest to Erp-BCA and CsBh-BCA, with a branch bootstrap value of 1.00 and pairwise sequence identity of 99 and 84, respectively, which indicates the possibility of horizontal gene transfer of  $\beta$ -CA coding genes in these microorganisms.

It should be noted that inorganic carbon from CO<sub>2</sub> is first obtained from the environment via diffusion through the plume, a branchial organ [147]. Next, CO<sub>2</sub> is transformed to HCO<sub>3</sub><sup>−</sup> and transported to trophosome cells, particularly bicarbonate, at the surrounding branchial plume interface. Then, HCO<sub>3</sub><sup>−</sup> is transformed to CO<sub>2</sub> on the body fluids and bacterial cells [148] and adhered via the bacterial symbiont enzyme RuBisCO form II. In the arginine biosynthesis and pyrimidine pathways, carbamylphosphate synthetase uses inorganic HCO<sub>3</sub><sup>−</sup> to start the biosynthesis process. Since the metabolic relationship between *R. pachyptila* and its endosymbiont is vital for the survival of each organism, this issue can explain the cause and importance of HGT of CA in these organisms. Furthermore, *R. pachyptila* contains an  $\alpha$ -CA gene [149] with UniProt ID: Q8MPH8, which is not similar to Erp-ACA.

Additionally, *T. jerichonana* has no reported CA family. Identification of the  $\beta$ -CA gene beside three transposase genes on one of the GIs of *H. crunogenus* SP-41 could lead to the theory that this gene may be transferred with plasmids and phages or occur through transposon accumulation in recombination sites. Experimental studies have suggested the release of about 1.5 billion symbionts from dead tubeworm clumps into the environment [47], which provides the opportunity for the spread and HGT of CA genes in the environment and preparing the biodiversity condition.

In addition to the  $\beta$ -CA phylogenetic tree, the heatmap showed that the Hc(SP41)-BCA in clade B is closely related to Hs(MA2-6)-BCA with a branch bootstrap value of 0.99 and a pairwise sequence identity value of 82.9. In addition, MeBa-BCA and MeBp-BCA showed a close relationship with Hc(SP41)-BCA with branch bootstrap values of 1.0 and pairwise sequence identity values of 76.56 for both cases. The HGT of hydrogenase-coding genes between *H. crunogenus* SP-41 and *H. crunogenus* XCL-2 was studied previously [150]; however, in this study, *H. crunogenus* SP-41 (*Hc(SP41)-BCA*) had no HGT relationship with *H. crunogenus* XCL-2. *R. pachyptila* has cytosolic  $\alpha$ -CA in the trophosome. Although these organisms need secretory CA for their physiological needs and use Erp-ACA, this theory must be experimentally studied.

The significance of this study revealed that there is an evolutionary relationship between Hc(XLC-2)ACA, Hc(SP41)-ACA, and Sca-ACA; G(HR-1)-ACA and G(EPR-M)-ACA; Sr-ACA and S(NBC37-1)-ACA; Pm-ACA and Ph-ACA; and CsBh-ACA and Erp-ACA in  $\alpha$ -CAs. In addition, there is an evolutionary relationship between Sr-BCA, S(NBC37)-BCA, and Si-BCA; Erp-BCA, Et-BCA, and CsBh-BCA; and Hts-BCA, Ts-BCA, Hc(XCL-2)-BCA, and Btt-BCA in  $\beta$ -CAs. Additionally, there is an evolutionary relationship between Erpi-GCA, Erp-GCA, and ET-GCA; Hts-GCA, Ts(S5)-GCA, and Sca-GCA; Gbah-GCA and Ggac-GCA; and Gs-GCA and Gk-GCA in  $\gamma$ -CAs.

Elevated CO<sub>2</sub> pressure in seawater can affect marine organisms by disrupting acid-base physiology and decreasing mineralization rates (affecting calcium carbonate saturation and calcification). Ocean uptake of anthropogenic CO<sub>2</sub> and associated changes in seawater

chemistry adversely affect biodiversity, other ecosystem processes, and the global carbon cycle [151]. The HGT and distribution of CA genes in the hydrothermal vent area may also help the survival and diversity of the organisms in this environment.

## 5. Conclusions

According to the results of this big data mining and bioinformatics study,  $\alpha$ -,  $\beta$ -, and  $\gamma$ -CAs from the thermophilic microbiome of marine hydrothermal vents have a reasonable evolutionary relationship. The  $\alpha$ -,  $\beta$ -, and  $\gamma$ -CA genes can be transferred to other microorganism habitats in hydrothermal vents via HGT and cause natural biodiversity in this extreme ecosystem. Given the presence of an integron with an integrase coding gene in the *Cycloclasticus* sp. symbiont of *Bathymodiolus heckeriae*, it is highly possible that the  $\alpha$ -CA coding gene is transferred between *Cycloclasticus* sp. as the symbiont of *B. heckeriae* and endosymbiont of *Riftia pachyptila*. This evolutionary phenomenon can also be applied to  $\beta$ -CA-coding genes.

According to the  $\beta$ -CA gene on the endosymbiont of *T. jerichonana* and the endosymbiont of *R. pachyptila* and the evolutionary relationship between them, the HGT of the  $\beta$ -CA gene from the endosymbiont of *T. jerichonana* to the endosymbiont of *R. pachyptila* and conversely is highly possible. In addition, the endosymbiont of *R. pachyptila* has a  $\gamma$ -CA gene on the chromosome; if  $\alpha$ - and  $\beta$ -CA coding genes are derived from other microorganisms, such as the endosymbiont of *T. jerichonana* and *Cycloclasticus* sp. as the symbiont of *B. heckeriae*, the theory of the necessity of the CA enzyme for survival in this extreme ecosystem and its effect on preserved natural biodiversity is proposed. Despite the presence of the  $\alpha$ -CA gene in *R. pachyptila* and the  $\alpha$ -,  $\beta$ -, and  $\gamma$ -CA genes in its endosymbiont, this theory is suggested for this giant marine worm. Therefore, the prokaryotic endosymbionts of mussels and giant marine worms have evolutionary relationships through HGT. With more focus on the HGT phenomenon, endosymbionts are integral parts of natural biodiversity and ecosystem functioning of marine hydrothermal vents.

**Supplementary Materials:** The following supporting information can be downloaded at: <https://www.mdpi.com/article/10.3390/biology12060770/s1>. Figure S1, Multiple Sequence Alignment of  $\alpha$ -CA from the thermophilic microbiome of hydrothermal vents; Figure S2, Multiple Sequence Alignment of  $\beta$ -CAs from the thermophilic microbiome of hydrothermal vents; Figure S3, Multiple Sequence Alignment of  $\gamma$ -CAs from the thermophilic microbiome of hydrothermal vents; Table S1,  $\alpha$ -CA proteins from the microbiome of marine hydrothermal vent ecosystems with taxonomic classifications; Table S2,  $\beta$ -CA proteins from the microbiome of marine hydrothermal vent ecosystems with taxonomic classifications; Table S3,  $\gamma$ -CA proteins from the microbiome of marine hydrothermal vent ecosystems with taxonomic classifications.

**Author Contributions:** M.S.G. performed the study and drafted the first version of this manuscript. R.Z.E., as the supervisor of this study, designed the study and edited the manuscript, figures, and tables. M.S.G., C.V.M., Ö.T.B., H.S.Z., S.P. and R.Z.E. performed further revisions on the manuscript. All authors have read and agreed to the published version of the manuscript.

**Funding:** The MSc thesis grant from NIGEB supported MSG. Also, RZE has been supported by grant No. 737 from NIGEB. In addition, to perform this study, RZE was supported by grant No. M/75137 from the Ministry of Science, Research, and Technology (MSRT) of the Islamic Republic of Iran based on the collaboration agreement between Iran and South Africa. In addition, OTB was supported by grant No. 111212 from the National Research Foundation (NRF) of South Africa. SP supported this study through his grants from the Jane and Aatos Erkko Foundation and the Academy of Finland, Finland.

**Institutional Review Board Statement:** Not applicable.

**Informed Consent Statement:** Not applicable.

**Data Availability Statement:** Not applicable.

**Acknowledgments:** We thank the National Institute of Genetic Engineering and Biotechnology (NIGEB) of the Islamic Republic of Iran and the National Research Foundation (NRF) of South Africa for preparing the conditions to perform this study. No funding organizations had any role in the design of the study; in the collection, analysis, or interpretation of data; in the writing of the manuscript; or in the decision to publish the results.

**Conflicts of Interest:** The authors declare that they have no known competing financial interests or personal relationships that could have appeared to influence the work reported in this paper.

## References

1. Lonsdale, P. Clustering of suspension-feeding macrobenthos near abyssal hydrothermal vents at oceanic spreading centers. *Deep Sea Res.* **1977**, *24*, 857–863. [[CrossRef](#)]
2. Corliss, J.B.; Dymond, J.; Gordon, L.I.; Edmond, J.M.; von Herzen, R.P.; Ballard, R.D.; Green, K.; Williams, D.; Bainbridge, A.; Crane, K. Submarine thermal springs on the Galapagos Rift. *Science* **1979**, *203*, 1073–1083. [[CrossRef](#)] [[PubMed](#)]
3. Colín-García, M.; Heredia, A.; Cordero, G.; Camprubí, A.; Negrón-Mendoza, A.; Ortega-Gutiérrez, F.; Beraldi, H.; Ramos-Bernal, S. Hydrothermal vents and prebiotic chemistry: A review. *Bol. Soc. Geol. Mex.* **2016**, *68*, 599–620. [[CrossRef](#)]
4. Shitashima, K. CO<sub>2</sub> supply from deep-sea hydrothermal systems. *Waste Manag.* **1998**, *17*, 385–390. [[CrossRef](#)]
5. Maren, T.H. Carbonic anhydrase: Chemistry, physiology, and inhibition. *Physiol. Rev.* **1967**, *47*, 595–781. [[CrossRef](#)]
6. Smith, K.S.; Jakubzick, C.; Whittam, T.S.; Ferry, J.G. Carbonic anhydrase is an ancient enzyme widespread in prokaryotes. *Proc. Natl. Acad. Sci. USA* **1999**, *96*, 15184–15189. [[CrossRef](#)]
7. Capasso, C.; Supuran, C.T. An overview of the alpha-, beta- and gamma-carbonic anhydrases from Bacteria: Can bacterial carbonic anhydrases shed new light on evolution of bacteria? *J. Enzym. Inhib. Med. Chem.* **2015**, *30*, 325–332. [[CrossRef](#)]
8. Zolfaghari Emameh, R.; Kuuslahti, M.; Näreaho, A.; Sukura, A.; Parkkila, S. Innovative molecular diagnosis of *T richinella* species based on  $\beta$ -carbonic anhydrase genomic sequence. *Microb. Biotechnol.* **2016**, *9*, 172–179. [[CrossRef](#)]
9. Zolfaghari Emameh, R.; Barker, H.R.; Syrjänen, L.; Urbański, L.; Supuran, C.T.; Parkkila, S. Identification and inhibition of carbonic anhydrases from nematodes. *J. Enzym. Inhib. Med. Chem.* **2016**, *31*, 176–184. [[CrossRef](#)]
10. Emameh, R.Z.; Kuuslahti, M.; Vullo, D.; Barker, H.R.; Supuran, C.T.; Parkkila, S. *Ascaris lumbricoides*  $\beta$  carbonic anhydrase: A potential target enzyme for treatment of ascariasis. *Parasites Vectors* **2015**, *8*, 479. [[CrossRef](#)]
11. Emameh, R.Z.; Barker, H.; Hytönen, V.P.; Tolvanen, M.E.; Parkkila, S. Beta carbonic anhydrases: Novel targets for pesticides and anti-parasitic agents in agriculture and livestock husbandry. *Parasites Vectors* **2014**, *7*, 403. [[CrossRef](#)] [[PubMed](#)]
12. Zolfaghari Emameh, R.; Kuuslahti, M.; Nosrati, H.; Lohi, H.; Parkkila, S. Assessment of databases to determine the validity of beta- and gamma-carbonic anhydrase sequences from vertebrates. *BMC Genom.* **2020**, *21*, 352. [[PubMed](#)]
13. Zolfaghari Emameh, R.; Hosseini, S.N.; Parkkila, S. Application of beta and gamma carbonic anhydrase sequences as tools for identification of bacterial contamination in the whole genome sequence of inbred Wuzhishan minipig (*Sus scrofa*) annotated in databases. *Database* **2021**, *2021*, baab029. [[PubMed](#)]
14. Lindskog, S. Structure and mechanism of carbonic anhydrase. *Pharmacol. Ther.* **1997**, *74*, 1–20. [[CrossRef](#)] [[PubMed](#)]
15. Akocak, S.; Supuran, C.T. Activation of  $\alpha$ -,  $\beta$ -,  $\gamma$ - $\delta$ -,  $\zeta$ - and  $\eta$ -class of carbonic anhydrases with amines and amino acids: A review. *J. Enzym. Inhib. Med. Chem.* **2019**, *34*, 1652–1659. [[CrossRef](#)]
16. Del Prete, S.; Nocentini, A.; Supuran, C.T.; Capasso, C. Bacterial  $\iota$ -carbonic anhydrase: A new active class of carbonic anhydrase identified in the genome of the Gram-negative bacterium *Burkholderia territorii*. *J. Enzym. Inhib. Med. Chem.* **2020**, *35*, 1060–1068. [[CrossRef](#)]
17. Supuran, C.T. Structure and function of carbonic anhydrases. *Biochem. J.* **2016**, *473*, 2023–2032. [[CrossRef](#)]
18. Supuran, C.T.; Capasso, C. An overview of the bacterial carbonic anhydrases. *Metabolites* **2017**, *7*, 56. [[CrossRef](#)]
19. Ferraroni, M.; Del Prete, S.; Vullo, D.; Capasso, C.; Supuran, C.T. Crystal structure and kinetic studies of a tetrameric type II  $\beta$ -carbonic anhydrase from the pathogenic bacterium *Vibrio cholerae*. *Acta Crystallogr. Sect. D Biol. Crystallogr.* **2015**, *71*, 2449–2456. [[CrossRef](#)]
20. Iverson, T.M.; Alber, B.E.; Kisker, C.; Ferry, J.G.; Rees, D.C. A closer look at the active site of  $\gamma$ -class carbonic anhydrases: High-resolution crystallographic studies of the carbonic anhydrase from *Methanosarcina thermophila*. *Biochemistry* **2000**, *39*, 9222–9231. [[CrossRef](#)]
21. Zolfaghari Emameh, R.; Barker, H.R.; Tolvanen, M.E.; Parkkila, S.; Hytönen, V.P. Horizontal transfer of  $\beta$ -carbonic anhydrase genes from prokaryotes to protozoans, insects, and nematodes. *Parasites Vectors* **2016**, *9*, 152. [[CrossRef](#)] [[PubMed](#)]
22. Emameh, R.Z.; Barker, H.R.; Hytönen, V.P.; Parkkila, S. Involvement of  $\beta$ -carbonic anhydrase genes in bacterial genomic islands and their horizontal transfer to protists. *Appl. Environ. Microbiol.* **2018**, *84*, e00771-18.
23. Andersson, J.O. Lateral gene transfer in eukaryotes. *Cell. Mol. Life Sci.* **2005**, *62*, 1182–1197. [[CrossRef](#)] [[PubMed](#)]
24. Emamalipour, M.; Seidi, K.; Zununi Vahed, S.; Jahanban-Esfahlan, A.; Jaymand, M.; Majidi, H.; Amoozgar, Z.; Chitkushev, L.; Javaheri, T.; Jahanban-Esfahlan, R. Horizontal gene transfer: From evolutionary flexibility to disease progression. *Front. Cell Dev. Biol.* **2020**, *8*, 229. [[CrossRef](#)] [[PubMed](#)]
25. Dutta, C.; Pan, A. Horizontal gene transfer and bacterial diversity. *J. Biosci.* **2002**, *27*, 27. [[CrossRef](#)] [[PubMed](#)]

26. Frost, L.S.; Leplae, R.; Summers, A.O.; Toussaint, A. Mobile genetic elements: The agents of open source evolution. *Nat. Rev. Microbiol.* **2005**, *3*, 722–732. [[CrossRef](#)]
27. Bellanger, X.; Payot, S.; Leblond-Bourget, N.; Guédon, G. Conjugative and mobilizable genomic islands in bacteria: Evolution and diversity. *FEMS Microbiol. Rev.* **2014**, *38*, 720–760. [[CrossRef](#)]
28. Johnson, C.M.; Grossman, A.D. Integrative and conjugative elements (ICEs): What they do and how they work. *Annu. Rev. Genet.* **2015**, *49*, 577–601. [[CrossRef](#)]
29. Watson, B.N.; Staals, R.H.; Fineran, P.C. CRISPR-Cas-mediated phage resistance enhances horizontal gene transfer by transduction. *mBio* **2018**, *9*, e02406-17. [[CrossRef](#)]
30. Muñoz-López, M.; García-Pérez, J.L. DNA transposons: Nature and applications in genomics. *Curr. Genom.* **2010**, *11*, 115–128. [[CrossRef](#)]
31. Thomas, C.M.; Nielsen, K.M. Mechanisms of, and barriers to, horizontal gene transfer between bacteria. *Nat. Rev. Microbiol.* **2005**, *3*, 711–721. [[CrossRef](#)] [[PubMed](#)]
32. Messier, N.; Roy, P.H. Integron integrases possess a unique additional domain necessary for activity. *J. Bacteriol.* **2001**, *183*, 6699–6706. [[CrossRef](#)] [[PubMed](#)]
33. Partridge, S.R.; Recchia, G.D.; Scaramuzzi, C.; Collis, C.M.; Stokes, H.; Hall, R.M. Definition of the attI1 site of class 1 integrons. *Microbiology* **2000**, *146*, 2855–2864. [[CrossRef](#)] [[PubMed](#)]
34. Collis, C.M.; Hall, R.M. Expression of antibiotic resistance genes in the integrated cassettes of integrons. *Antimicrob. Agents Chemother.* **1995**, *39*, 155–162. [[CrossRef](#)]
35. Alvarez-Martinez, C.E.; Christie, P.J. Biological diversity of prokaryotic type IV secretion systems. *Microbiol. Mol. Biol. Rev.* **2009**, *73*, 775–808. [[CrossRef](#)]
36. Domsic, J.F.; McKenna, R. Sequestration of carbon dioxide by the hydrophobic pocket of the carbonic anhydrases. *Biochim. Biophys. Acta-Proteins Proteom.* **2010**, *1804*, 326–331. [[CrossRef](#)]
37. Mahillon, J.; Chandler, M. Insertion sequences. *Microbiol. Mol. Biol. Rev.* **1998**, *62*, 725–774. [[CrossRef](#)]
38. Fisher, R.M.; Henry, L.M.; Cornwallis, C.K.; Kiers, E.T.; West, S.A. The evolution of host-symbiont dependence. *Nat. Commun.* **2017**, *8*, 15973. [[CrossRef](#)]
39. Hall, R.J.; Whelan, F.J.; McInerney, J.O.; Ou, Y.; Domingo-Sananes, M.R. Horizontal Gene Transfer as a Source of Conflict and Cooperation in Prokaryotes. *Front Microbiol* **2020**, *11*, 1569.
40. Sabine, C.L.; Tanhua, T. Estimation of anthropogenic CO<sub>2</sub> inventories in the ocean. *Ann. Rev. Mar. Sci.* **2010**, *2*, 175–198. [[CrossRef](#)]
41. De Goeyse, S.; Webb, A.E.; Reichart, G.-J.; De Nooijer, L.J. Carbonic anhydrase is involved in calcification by the benthic foraminifer *Ammonia lessona*. *Biogeosciences* **2021**, *18*, 393–401. [[CrossRef](#)]
42. Manyumwa, C.V.; Emameh, R.Z.; Tasthan Bishop, Ö. Alpha-carbonic anhydrases from hydrothermal vent sources as potential carbon dioxide sequestration agents: In silico sequence, structure and dynamics analyses. *Int. J. Mol. Sci.* **2020**, *21*, 8066. [[CrossRef](#)] [[PubMed](#)]
43. Cardoso, J.C.; Ferreira, V.; Zhang, X.; Anjos, L.; Félix, R.C.; Batista, F.M.; Power, D.M. Evolution and diversity of alpha-carbonic anhydrases in the mantle of the Mediterranean mussel (*Mytilus galloprovincialis*). *Sci. Rep.* **2019**, *9*, 10400. [[CrossRef](#)] [[PubMed](#)]
44. Parisi, G.; Perales, M.; Fornasari, M.; Colaneri, A.; Schain, N.; Casati, D.; Zimmermann, S.; Brennicke, A.; Araya, A.; Ferry, J. Gamma carbonic anhydrases in plant mitochondria. *Plant Mol. Biol.* **2004**, *55*, 193–207. [[CrossRef](#)]
45. Smith, K.S.; Ferry, J.G. Prokaryotic carbonic anhydrases. *FEMS Microbiol. Rev.* **2000**, *24*, 335–366. [[CrossRef](#)]
46. Dobrinski, K.P.; Longo, D.L.; Scott, K.M. The carbon-concentrating mechanism of the hydrothermal vent chemolithoautotroph *Thiomicrospira crunogena*. *J. Bacteriol.* **2005**, *187*, 5761–5766. [[CrossRef](#)]
47. Miroshnichenko, M.L.; Kostrikina, N.A.; Chernyh, N.A.; Pimenov, N.V.; Tourova, T.P.; Antipov, A.N.; Spring, S.; Stackebrandt, E.; Bonch-Osmolovskaya, E.A. *Caldithrix abyssi* gen. nov., sp. nov., a nitrate-reducing, thermophilic, anaerobic bacterium isolated from a Mid-Atlantic Ridge hydrothermal vent, represents a novel bacterial lineage. *Int. J. Syst. Evol. Microbiol.* **2003**, *53*, 323–329. [[CrossRef](#)]
48. Voordeckers, J.W.; Starovoytov, V.; Vetriani, C. *Caminibacter mediatlanticus* sp. nov., a thermophilic, chemolithoautotrophic, nitrate-ammonifying bacterium isolated from a deep-sea hydrothermal vent on the Mid-Atlantic Ridge. *Int. J. Syst. Evol. Microbiol.* **2005**, *55*, 773–779. [[CrossRef](#)]
49. Ward, M.E.; Shields, J.D.; Van Dover, C.L. Parasitism in species of *Bathymodiolus* (Bivalvia: Mytilidae) mussels from deep-sea seep and hydrothermal vents. *Dis. Aquat.* **2004**, *62*, 1–16. [[CrossRef](#)]
50. Klose, J.; Polz, M.F.; Wagner, M.; Schimak, M.P.; Gollner, S.; Bright, M. Endosymbionts escape dead hydrothermal vent tubeworms to enrich the free-living population. *Proc. Natl. Acad. Sci. USA* **2015**, *112*, 11300–11305. [[CrossRef](#)]
51. L’Haridon, S.; Reysenbach, A.-L.; Tindall, B.; Schönheit, P.; Banta, A.; Johnsen, U.; Schumann, P.; Gambacorta, A.; Stackebrandt, E.; Jeannot, C. *Desulfurobacterium atlanticum* sp. nov., *Desulfurobacterium pacificum* sp. nov. and *Thermovibrio guaymasensis* sp. nov., three thermophilic members of the Desulfurobacteriaceae fam. nov., a deep branching lineage within the Bacteria. *Int. J. Syst. Evol. Microbiol.* **2006**, *56*, 2843–2852. [[CrossRef](#)] [[PubMed](#)]
52. Hansen, M.; Perner, M. Reasons for *Thiomicrospira crunogena*’s recalcitrance towards previous attempts to detect its hydrogen consumption ability. *Environ. Microbiol. Rep.* **2016**, *8*, 53–57. [[CrossRef](#)]



53. Takai, K.; Nealson, K.H.; Horikoshi, K. *Hydrogenimonas thermophila* gen. nov., sp. nov., a novel thermophilic, hydrogen-oxidizing chemolithoautotroph within the  $\epsilon$ -Proteobacteria, isolated from a black smoker in a Central Indian Ridge hydrothermal field. *Int. J. Syst. Evol. Microbiol.* **2004**, *54*, 25–32. [[CrossRef](#)] [[PubMed](#)]
54. Mino, S.; Shiotani, T.; Nakagawa, S.; Takai, K.; Sawabe, T. *Hydrogenimonas urashimensis* sp. nov., a hydrogen-oxidizing chemolithoautotroph isolated from a deep-sea hydrothermal vent in the Southern Mariana Trough. *Syst. Appl. Microbiol.* **2021**, *44*, 126170. [[CrossRef](#)] [[PubMed](#)]
55. Shiotani, T.; Mino, S.; Sato, W.; Nishikawa, S.; Yonezawa, M.; Sievert, S.M.; Sawabe, T. *Nitrosophilus alvini* gen. nov., sp. nov., a hydrogen-oxidizing chemolithoautotroph isolated from a deep-sea hydrothermal vent in the East Pacific Rise, inferred by a genome-based taxonomy of the phylum “Campylobacterota”. *PLoS ONE* **2020**, *15*, e0241366. [[CrossRef](#)]
56. Nakagawa, S.; Takai, K.; Inagaki, F.; Horikoshi, K.; Sako, Y. *Nitratiruptor tergaricus* gen. nov., sp. nov. and *Nitratifactor salsuginis* gen. nov., sp. nov., nitrate-reducing chemolithoautotrophs of the  $\epsilon$ -Proteobacteria isolated from a deep-sea hydrothermal system in the Mid-Okinawa Trough. *Int. J. Syst. Evol. Microbiol.* **2005**, *55*, 925–933. [[CrossRef](#)]
57. François, D.X.; Godfroy, A.; Mathien, C.; Aubé, J.; Cathalot, C.; Lesongeur, F.; L’Haridon, S.; Philippon, X.; Roussel, E.G. *Persephonella atlantica* sp. nov.: How to adapt to physico-chemical gradients in high temperature hydrothermal habitats. *Syst. Appl. Microbiol.* **2021**, *44*, 126176. [[CrossRef](#)]
58. Nakagawa, S.; Takai, K.; Horikoshi, K.; Sako, Y. *Persephonella hydrogeniphila* sp. nov., a novel thermophilic, hydrogen-oxidizing bacterium from a deep-sea hydrothermal vent chimney. *Int. J. Syst. Evol. Microbiol.* **2003**, *53*, 863–869. [[CrossRef](#)]
59. Götz, D.; Banta, A.; Beveridge, T.; Rushdi, A.; Simoneit, B.; Reysenbach, A. *Persephonella marina* gen. nov., sp. nov. and *Persephonella guaymasensis* sp. nov., two novel, thermophilic, hydrogen-oxidizing microaerophiles from deep-sea hydrothermal vents. *Int. J. Syst. Evol. Microbiol.* **2002**, *52*, 1349–1359.
60. Waite, D.W.; Vanwonterghem, I.; Rinke, C.; Parks, D.H.; Zhang, Y.; Takai, K.; Sievert, S.M.; Simon, J.; Campbell, B.J.; Hanson, T.E. Comparative genomic analysis of the class Epsilonproteobacteria and proposed reclassification to Epsilonbacteraeota (phyl. nov.). *Front. Microbiol.* **2017**, *8*, 682. [[CrossRef](#)]
61. Xie, S.; Wang, S.; Li, D.; Shao, Z.; Lai, Q.; Wang, Y.; Wei, M.; Han, X.; Jiang, L. *Sulfurovum indicum* sp. nov., a novel hydrogen-and sulfur-oxidizing chemolithoautotroph isolated from a deep-sea hydrothermal plume in the Northwestern Indian Ocean. *Int. J. Syst. Evol. Microbiol.* **2021**, *71*, 004748. [[CrossRef](#)] [[PubMed](#)]
62. Takai, K.; Suzuki, M.; Nakagawa, S.; Miyazaki, M.; Suzuki, Y.; Inagaki, F.; Horikoshi, K. *Sulfurimonas paralvinellae* sp. nov., a novel mesophilic, hydrogen-and sulfur-oxidizing chemolithoautotroph within the Epsilonproteobacteria isolated from a deep-sea hydrothermal vent polychaete nest, reclassification of *Thiomicrospira denitrificans* as *Sulfurimonas denitrificans* comb. nov. and emended description of the genus *Sulfurimonas*. *Int. J. Syst. Evol. Microbiol.* **2006**, *56*, 1725–1733. [[PubMed](#)]
63. Boutet, I.; Ripp, R.; Lecompte, O.; Dossat, C.; Corre, E.; Tanguy, A.; Lallier, F.H. Conjugating effects of symbionts and environmental factors on gene expression in deep-sea hydrothermal vent mussels. *BMC Genom.* **2011**, *12*, 530. [[CrossRef](#)] [[PubMed](#)]
64. Poli, A.; Gugliandolo, C.; Spanò, A.; Taurisano, V.; Di Donato, P.; Maugeri, T.L.; Nicolaus, B.; Arena, A. Poly-[Gamma]-Glutamic Acid from *Bacillus Horneckiae* Strain APA of Shallow Marine Vent Origin with Antiviral and Immunomodulatory Effects against Herpes Simplex Virus Type-2. *J. Mar. Sci. Res. Dev.* **2015**, *5*, 173. [[CrossRef](#)]
65. Wu, Y.-H.; Xu, L.; Zhou, P.; Wang, C.-S.; Oren, A.; Xu, X.-W. *Brevirhabdus pacifica* gen. nov., sp. nov., isolated from deep-sea sediment in a hydrothermal vent field. *Int. J. Syst. Evol. Microbiol.* **2015**, *65*, 3645–3651. [[CrossRef](#)]
66. Ponnudurai, R.; Sayavedra, L.; Kleiner, M.; Heiden, S.E.; Thürmer, A.; Felbeck, H.; Schlüter, R.; Sievert, S.M.; Daniel, R.; Schweder, T. Genome sequence of the sulfur-oxidizing *Bathymodiolus thermophilus* gill endosymbiont. *Stand. Genom. Sci.* **2017**, *12*, 50. [[CrossRef](#)]
67. Grosche, A.; Sekaran, H.; Pérez-Rodríguez, I.; Starovoytov, V.; Vetriani, C. *Cetia pacifica* gen. nov., sp. nov., a chemolithoautotrophic, thermophilic, nitrate-ammonifying bacterium from a deep-sea hydrothermal vent. *Int. J. Syst. Evol. Microbiol.* **2015**, *65*, 1144–1150. [[CrossRef](#)]
68. Slobodkina, G.; Kolganova, T.; Chernyh, N.; Querellou, J.; Bonch-Osmolovskaya, E.; Slobodkin, A. *Deferribacter autotrophicus* sp. nov., an iron (III)-reducing bacterium from a deep-sea hydrothermal vent. *Int. J. Syst. Evol. Microbiol.* **2009**, *59*, 1508–1512. [[CrossRef](#)]
69. Cao, J.; Birien, T.; Gayet, N.; Huang, Z.; Shao, Z.; Jebbar, M.; Alain, K. *Desulfurobacterium indicum* sp. nov., a thermophilic sulfur-reducing bacterium from the Indian Ocean. *Int. J. Syst. Evol. Microbiol.* **2017**, *67*, 1665–1668. [[CrossRef](#)]
70. Jiang, L.; Xu, H.; Shao, Z.; Long, M. *Defluviimonas indica* sp. nov., a marine bacterium isolated from a deep-sea hydrothermal vent environment. *Int. J. Syst. Evol. Microbiol.* **2014**, *64*, 2084–2088. [[CrossRef](#)]
71. Hansen, M.; Perner, M. Hydrogenase gene distribution and H<sub>2</sub> consumption ability within the *Thiomicrospira* lineage. *Front. Microbiol.* **2016**, *7*, 99. [[CrossRef](#)] [[PubMed](#)]
72. Kaye, J.Z.; Marquez, M.C.; Ventosa, A.; Baross, J.A. *Halomonas neptunia* sp. nov., *Halomonas sulfidaeris* sp. nov., *Halomonas axialensis* sp. nov. and *Halomonas hydrothermalis* sp. nov.: Halophilic bacteria isolated from deep-sea hydrothermal-vent environments. *Int. J. Syst. Evol. Microbiol.* **2004**, *54*, 499–511. [[CrossRef](#)] [[PubMed](#)]
73. Jiang, L.; Lyu, J.; Shao, Z. Sulfur metabolism of *Hydrogenovibrio thermophilus* strain S5 and its adaptations to deep-sea hydrothermal vent environment. *Front. Microbiol.* **2017**, *8*, 2513. [[CrossRef](#)] [[PubMed](#)]

74. Slobodkina, G.B.; Baslerov, R.V.; Novikov, A.A.; Viryasov, M.B.; Bonch-Osmolovskaya, E.A.; Slobodkin, A.I. *Inmirania thermophilica* gen. nov., sp. nov., a thermophilic, facultatively autotrophic, sulfur-oxidizing gammaproteobacterium isolated from a shallow-sea hydrothermal vent. *Int. J. Syst. Evol. Microbiol.* **2016**, *66*, 701–706. [[CrossRef](#)]
75. Nagata, R.; Takaki, Y.; Tame, A.; Nunoura, T.; Muto, H.; Mino, S.; Sawayama, S.; Takai, K.; Nakagawa, S. *Lebetimonas natsushimae* sp. nov., a novel strictly anaerobic, moderately thermophilic chemoautotroph isolated from a deep-sea hydrothermal vent polychaete nest in the Mid-Okinawa Trough. *Syst. Appl. Microbiol.* **2017**, *40*, 352–356. [[CrossRef](#)]
76. Stewart, L.C.; Jung, J.-H.; Kim, Y.-T.; Kwon, S.-W.; Park, C.-S.; Holden, J.F. *Methanocaldococcus bathoardescens* sp. nov., a hyperthermophilic methanogen isolated from a volcanically active deep-sea hydrothermal vent. *Int. J. Syst. Evol. Microbiol.* **2015**, *65*, 1280–1283. [[CrossRef](#)]
77. McAllister, S.M.; Davis, R.E.; McBeth, J.M.; Tebo, B.M.; Emerson, D.; Moyer, C.L. Biodiversity and emerging biogeography of the neutrophilic iron-oxidizing Zetaproteobacteria. *Appl. Environ. Microbiol.* **2011**, *77*, 5445–5457. [[CrossRef](#)]
78. Takai, K.; Nealson, K.H.; Horikoshi, K. *Methanotorris formicicus* sp. nov., a novel extremely thermophilic, methane-producing archaeon isolated from a black smoker chimney in the Central Indian Ridge. *Int. J. Syst. Evol. Microbiol.* **2004**, *54*, 1095–1100. [[CrossRef](#)]
79. Takeuchi, M.; Katayama, T.; Yamagishi, T.; Hanada, S.; Tamaki, H.; Kamagata, Y.; Oshima, K.; Hattori, M.; Marumo, K.; Nedachi, M. *Methyloceanibacter caenitepidi* gen. nov., sp. nov., a facultatively methylotrophic bacterium isolated from marine sediments near a hydrothermal vent. *Int. J. Syst. Evol. Microbiol.* **2014**, *64*, 462–468. [[CrossRef](#)]
80. Wang, H.; Li, H.; Shao, Z.; Liao, S.; Johnstone, L.; Rensing, C.; Wang, G. Genome sequence of deep-sea manganese-oxidizing bacterium *Marinobacter manganoxydans* MnI7-9. *J. Bacteriol.* **2012**, *194*, 899–900. [[CrossRef](#)]
81. Takai, K.; Inoue, A.; Horikoshi, K. *Methanothermococcus okinawensis* sp. nov., a thermophilic, methane-producing archaeon isolated from a Western Pacific deep-sea hydrothermal vent system. *Int. J. Syst. Evol. Microbiol.* **2002**, *52*, 1089–1095. [[PubMed](#)]
82. Zhou, M.; Dong, B.; Shao, Z. Complete genome sequence of *Marinobacter* sp. LQ44, a haloalkaliphilic phenol-degrading bacterium isolated from a deep-sea hydrothermal vent. *Mar. Genom.* **2020**, *50*, 100697. [[CrossRef](#)]
83. Handley, K.M.; Hery, M.; Lloyd, J.R. *Marinobacter santoriniensis* sp. nov., an arsenate-respiring and arsenite-oxidizing bacterium isolated from hydrothermal sediment. *Int. J. Syst. Evol. Microbiol.* **2009**, *59*, 886–892. [[CrossRef](#)] [[PubMed](#)]
84. Smith, J.L.; Campbell, B.J.; Hanson, T.E.; Zhang, C.L.; Cary, S.C. *Nautilia profundicola* sp. nov., a thermophilic, sulfur-reducing epsilonproteobacterium from deep-sea hydrothermal vents. *Int. J. Syst. Evol. Microbiol.* **2008**, *58*, 1598–1602. [[CrossRef](#)]
85. Dong, C.; Lai, Q.; Chen, L.; Sun, F.; Shao, Z.; Yu, Z. *Oceanibaculum pacificum* sp. nov., isolated from hydrothermal field sediment of the south-west Pacific Ocean. *Int. J. Syst. Evol. Microbiol.* **2010**, *60*, 219–222. [[CrossRef](#)]
86. Miroschnichenko, M.; L'haridon, S.; Jeanthon, C.; Antipov, A.; Kostrikina, N.; Tindall, B.; Schumann, P.; Spring, S.; Stackebrandt, E.; Bonch-Osmolovskaya, E. *Oceanithermus profundus* gen. nov., sp. nov., a thermophilic, microaerophilic, facultatively chemolithoheterotrophic bacterium from a deep-sea hydrothermal vent. *Int. J. Syst. Evol. Microbiol.* **2003**, *53*, 747–752. [[CrossRef](#)]
87. Newton, I.; Woyke, T.; Auchtung, T.; Dilly, G.; Dutton, R.; Fisher, M.; Fontanez, K.; Lau, E.; Stewart, F.; Richardson, P. The *Calyptogenia magnifica* chemoautotrophic symbiont genome. *Science* **2007**, *315*, 998–1000. [[CrossRef](#)]
88. Guo, W.; Zhang, H.; Zhou, W.; Wang, Y.; Zhou, H.; Chen, X. Sulfur metabolism pathways in *Sulfobacillus acidophilus* TPY, a gram-positive moderate thermoacidophile from a hydrothermal vent. *Front. Microbiol.* **2016**, *7*, 1861. [[CrossRef](#)]
89. Inagaki, F.; Takai, K.; Nealson, K.H.; Horikoshi, K. *Sulfurovum lithotrophicum* gen. nov., sp. nov., a novel sulfur-oxidizing chemolithoautotroph within the  $\epsilon$ -Proteobacteria isolated from Okinawa Trough hydrothermal sediments. *Int. J. Syst. Evol. Microbiol.* **2004**, *54*, 1477–1482. [[CrossRef](#)]
90. Giovannelli, D.; Chung, M.; Staley, J.; Starovoytov, V.; Le Bris, N.; Vetriani, C. *Sulfurovum riftiae* sp. nov., a mesophilic, thiosulfate-oxidizing, nitrate-reducing chemolithoautotrophic epsilonproteobacterium isolated from the tube of the deep-sea hydrothermal vent polychaete *Riftia pachyptila*. *Int. J. Syst. Evol. Microbiol.* **2016**, *66*, 2697–2701. [[CrossRef](#)]
91. Vetriani, C.; Speck, M.D.; Ellor, S.V.; Lutz, R.A.; Starovoytov, V. *Thermovibrio ammonificans* sp. nov., a thermophilic, chemolithotrophic, nitrate-ammonifying bacterium from deep-sea hydrothermal vents. *Int. J. Syst. Evol. Microbiol.* **2004**, *54*, 175–181. [[CrossRef](#)] [[PubMed](#)]
92. Urios, L.; Cuffey, V.; Pignet, P.; Barbier, G. *Tepidibacter formicigenes* sp. nov., a novel spore-forming bacterium isolated from a Mid-Atlantic Ridge hydrothermal vent. *Int. J. Syst. Evol. Microbiol.* **2004**, *54*, 439–443. [[CrossRef](#)] [[PubMed](#)]
93. Hensley, S.A.; Jung, J.-H.; Park, C.-S.; Holden, J.F. *Thermococcus paralvinellae* sp. nov. and *Thermococcus cleftensis* sp. nov. of hyperthermophilic heterotrophs from deep-sea hydrothermal vents. *Int. J. Syst. Evol. Microbiol.* **2014**, *64*, 3655–3659. [[CrossRef](#)]
94. Martins, E.; Santos, R.S.; Bettencourt, R. *Vibrio diabolicus* challenge in *Bathymodiulus azoricus* populations from Menez Gwen and Lucky Strike hydrothermal vent sites. *Fish. Shellfish Immunol.* **2015**, *47*, 962–977. [[CrossRef](#)] [[PubMed](#)]
95. Kuwahara, H.; Yoshida, T.; Takaki, Y.; Shimamura, S.; Nishi, S.; Harada, M.; Matsuyama, K.; Takishita, K.; Kawato, M.; Uematsu, K. Reduced genome of the thioautotrophic intracellular symbiont in a deep-sea clam, *Calyptogenia okutanii*. *Curr. Biol.* **2007**, *17*, 881–886. [[CrossRef](#)] [[PubMed](#)]
96. Zeng, X.; Zhang, Z.; Li, X.; Zhang, X.; Cao, J.; Jebbar, M.; Alain, K.; Shao, Z. *Anoxybacter fermentans* gen. nov., sp. nov., a piezophilic, thermophilic, anaerobic, fermentative bacterium isolated from a deep-sea hydrothermal vent. *Int. J. Syst. Evol. Microbiol.* **2015**, *65*, 710–715. [[CrossRef](#)] [[PubMed](#)]

97. Zammuto, V.; Fuchs, F.M.; Fiebrandt, M.; Stapelmann, K.; Ulrich, N.J.; Maugeri, T.L.; Pukall, R.; Gugliandolo, C.; Moeller, R. Comparing spore resistance of *Bacillus* strains isolated from hydrothermal vents and spacecraft assembly facilities to environmental stressors and decontamination treatments. *Astrobiology* **2018**, *18*, 1425–1434. [[CrossRef](#)]
98. Wery, N.; Moricet, J.-M.; Cueff, V.; Jean, J.; Pignet, P.; Lesongeur, F.; Cambon-Bonavita, M.-A.; Barbier, G. *Caloranaerobacter azorensis* gen. nov., sp. nov., an anaerobic thermophilic bacterium isolated from a deep-sea hydrothermal vent. *Int. J. Syst. Evol. Microbiol.* **2001**, *51*, 1789–1796. [[CrossRef](#)]
99. Alain, K.; Pignet, P.; Zbinden, M.; Quillevère, M.; Duchiron, F.; Donval, J.-P.; Lesongeur, F.; Raguènes, G.; Crassous, P.; Querellou, J. *Caminicella sporogenes* gen. nov., sp. nov., a novel thermophilic spore-forming bacterium isolated from an East-Pacific Rise hydrothermal vent. *Int. J. Syst. Evol. Microbiol.* **2002**, *52*, 1621–1628.
100. Takai, K.; Kobayashi, H.; Nealson, K.H.; Horikoshi, K. *Deferribacter desulfuricans* sp. nov., a novel sulfur-, nitrate- and arsenate-reducing thermophile isolated from a deep-sea hydrothermal vent. *Int. J. Syst. Evol. Microbiol.* **2003**, *53*, 839–846. [[CrossRef](#)]
101. Chao, L.S.L.; Davis, R.E.; Moyer, C.L. Characterization of bacterial community structure in vestimentiferan tubeworm *Ridgeia piscesae* trophosomes. *Mar. Ecol.* **2007**, *28*, 72–85. [[CrossRef](#)]
102. Won, Y.-J.; Hallam, S.J.; O'Mullan, G.D.; Pan, I.L.; Buck, K.R.; Vrijenhoek, R.C. Environmental acquisition of thiotrophic endosymbionts by deep-sea mussels of the genus *Bathymodiolus*. *Appl. Environ. Microbiol.* **2003**, *69*, 6785–6792. [[CrossRef](#)] [[PubMed](#)]
103. Slobodkina, G.; Kolganova, T.; Querellou, J.; Bonch-Osmolovskaya, E.; Slobodkin, A. *Geoglobus acetivorans* sp. nov., an iron (III)-reducing archaeon from a deep-sea hydrothermal vent. *Int. J. Syst. Evol. Microbiol.* **2009**, *59*, 2880–2883. [[CrossRef](#)]
104. Maugeri, T.L.; Gugliandolo, C.; Caccamo, D.; Stackebrandt, E. Three novel halotolerant and thermophilic *Geobacillus* strains from shallow marine vents. *Syst. Appl. Microbiol.* **2002**, *25*, 450–455. [[CrossRef](#)] [[PubMed](#)]
105. Roalkvam, I.; Bredy, F.; Baumberger, T.; Pedersen, R.-B.; Steen, I.H. *Hypnocyclicus thermotrophus* gen. nov., sp. nov. isolated from a microbial mat in a hydrothermal vent field. *Int. J. Syst. Evol. Microbiol.* **2015**, *65*, 4521–4525. [[CrossRef](#)]
106. Van Dover, C. *The Ecology of Deep-Sea Hydrothermal Vents*; Princeton University Press: Princeton, NJ, USA, 2000.
107. Erauso, G.; Reysenbach, A.-L.; Godfroy, A.; Meunier, J.-R.; Crump, B.; Partensky, F.; Baross, J.A.; Marteinsson, V.; Barbier, G.; Pace, N.R. *Pyrococcus abyssi* sp. nov., a new hyperthermophilic archaeon isolated from a deep-sea hydrothermal vent. *Arch. Microbiol.* **1993**, *160*, 338–349. [[CrossRef](#)]
108. Marteinsson, V.T.; Bjornsdottir, S.H.; Bienvenu, N.; Kristjansson, J.K.; Birrien, J.-L. *Rhodothermus profundus* sp. nov., a thermophilic bacterium isolated from a deep-sea hydrothermal vent in the Pacific Ocean. *Int. J. Syst. Evol. Microbiol.* **2010**, *60*, 2729–2734. [[CrossRef](#)]
109. Miroshnichenko, M.; Gongadze, G.; Rainey, F.; Kostyukova, A.; Lysenko, A.; Chernyh, N.; Bonch-Osmolovskaya, E. *Thermococcus gorgonarius* sp. nov. and *Thermococcus pacificus* sp. nov.: Heterotrophic extremely thermophilic archaea from New Zealand submarine hot vents. *Int. J. Syst. Evol. Microbiol.* **1998**, *48*, 23–29. [[CrossRef](#)]
110. Marteinsson, V.T.; Birrien, J.-L.; Reysenbach, A.-L.; Vernet, M.; Marie, D.; Gambacorta, A.; Messner, P.; Sleytr, U.B.; Prieur, D. *Thermococcus barophilus* sp. nov., a new barophilic and hyperthermophilic archaeon isolated under high hydrostatic pressure from a deep-sea hydrothermal vent. *Int. J. Syst. Evol. Microbiol.* **1999**, *49*, 351–359. [[CrossRef](#)]
111. Duffaud, G.D.; d'Hennezel, O.B.; Peek, A.S.; Reysenbach, A.-L.; Kelly, R.M. Isolation and characterization of *Thermococcus barossii*, sp. nov., a hyperthermophilic archaeon isolated from a hydrothermal vent flange formation. *Syst. Appl. Microbiol.* **1998**, *21*, 40–49. [[CrossRef](#)]
112. Jolivet, E.; L'Haridon, S.; Corre, E.; Forterre, P.; Prieur, D. *Thermococcus gammatolerans* sp. nov., a hyperthermophilic archaeon from a deep-sea hydrothermal vent that resists ionizing radiation. *Int. J. Syst. Evol. Microbiol.* **2003**, *53*, 847–851. [[CrossRef](#)]
113. Gorlas, A.; Croce, O.; Oberto, J.; Gauliard, E.; Forterre, P.; Marguet, E. *Thermococcus nautili* sp. nov., a hyperthermophilic archaeon isolated from a hydrothermal deep-sea vent. *Int. J. Syst. Evol. Microbiol.* **2014**, *64*, 1802–1810. [[CrossRef](#)] [[PubMed](#)]
114. González, J.M.; Kato, C.; Horikoshi, K. *Thermococcus peptonophilus* sp. nov., a fast-growing, extremely thermophilic archaeobacterium isolated from deep-sea hydrothermal vents. *Arch. Microbiol.* **1995**, *164*, 159–164. [[CrossRef](#)] [[PubMed](#)]
115. Kobayashi, T.; Kwak, Y.S.; Akiba, T.; Kudo, T.; Horikoshi, K. *Thermococcus profundus* sp. nov., a new hyperthermophilic archaeon isolated from a deep-sea hydrothermal vent. *Syst. Appl. Microbiol.* **1994**, *17*, 232–236. [[CrossRef](#)]
116. Dalmasso, C.; Oger, P.; Selva, G.; Courtine, D.; L'haridon, S.; Garlaschelli, A.; Roussel, E.; Miyazaki, J.; Reveillaud, J.; Jebbar, M. *Thermococcus piezophilus* sp. nov., a novel hyperthermophilic and piezophilic archaeon with a broad pressure range for growth, isolated from a deepest hydrothermal vent at the Mid-Cayman Rise. *Syst. Appl. Microbiol.* **2016**, *39*, 440–444. [[CrossRef](#)] [[PubMed](#)]
117. Slobodkin, A.; Tourova, T.; Kostrikina, N.; Chernyh, N.; Bonch-Osmolovskaya, E.; Jeanthon, C.; Jones, B. *Tepidibacter thalassicus* gen. nov., sp. nov., a novel moderately thermophilic, anaerobic, fermentative bacterium from a deep-sea hydrothermal vent. *J. Med. Microbiol.* **2003**, *53*, 1131–1134.
118. L'Haridon, S.; Miroshnichenko, M.; Kostrikina, N.; Tindall, B.; Spring, S.; Schumann, P.; Stackebrandt, E.; Bonch-Osmolovskaya, E.; Jeanthon, C. *Vulcanibacillus modesticaldus* gen. nov., sp. nov., a strictly anaerobic, nitrate-reducing bacterium from deep-sea hydrothermal vents. *Int. J. Syst. Evol. Microbiol.* **2006**, *56*, 1047–1053. [[CrossRef](#)]
119. Notredame, C.; Higgins, D.G.; Heringa, J. T-Coffee: A novel method for fast and accurate multiple sequence alignment. *J. Mol. Biol.* **2000**, *302*, 205–217. [[CrossRef](#)] [[PubMed](#)]
120. Waterhouse, A.M.; Procter, J.B.; Martin, D.M.; Clamp, M.; Barton, G.J. Jalview Version 2—A multiple sequence alignment editor and analysis workbench. *Bioinformatics* **2009**, *25*, 1189–1191. [[CrossRef](#)]

121. Nei, M.; Kumar, S. *Molecular Evolution and Phylogenetics*; Oxford University Press: New York, NY, USA, 2000.
122. Kumar, S.; Stecher, G.; Li, M.; Niyaz, C.; Tamura, K. MEGA X: Molecular evolutionary genetics analysis across computing platforms. *Mol. Biol. Evol.* **2018**, *35*, 1547–1549. [[CrossRef](#)]
123. Hall, R.M.; Brookes, D.E.; Stokes, H. Site-specific insertion of genes into integrons: Role of the 59-base element and determination of the recombination cross-over point. *Mol. Microbiol.* **1991**, *5*, 1941–1959. [[CrossRef](#)] [[PubMed](#)]
124. Rowe-Magnus, D.A.; Guérout, A.-M.; Mazel, D. Super-integrons. *Res. Microbiol.* **1999**, *150*, 641–651. [[CrossRef](#)] [[PubMed](#)]
125. Rowe-Magnus, D.A.; Guerout, A.-M.; Ploncard, P.; Dychinco, B.; Davies, J.; Mazel, D. The evolutionary history of chromosomal super-integrons provides an ancestry for multiresistant integrons. *Proc. Natl. Acad. Sci. USA* **2001**, *98*, 652–657. [[CrossRef](#)] [[PubMed](#)]
126. Stokes, H.; O’Gorman, D.; Recchia, G.D.; Parsekhian, M.; Hall, R.M. Structure and function of 59-base element recombination sites associated with mobile gene cassettes. *Mol. Microbiol.* **1997**, *26*, 731–745. [[CrossRef](#)]
127. Collis, C.M.; Hall, R.M. Gene cassettes from the insert region of integrons are excised as covalently closed circles. *Mol. Microbiol.* **1992**, *6*, 2875–2885. [[CrossRef](#)]
128. Hocquet, D.; Llanes, C.; Thouverez, M.; Kulasekara, H.D.; Bertrand, X.; Plésiat, P.; Mazel, D.; Miller, S.I. Evidence for induction of integron-based antibiotic resistance by the SOS response in a clinical setting. *PLoS Pathog.* **2012**, *8*, e1002778. [[CrossRef](#)]
129. Cury, J.; Jové, T.; Touchon, M.; Néron, B.; Rocha, E.P. Identification and analysis of integrons and cassette arrays in bacterial genomes. *Nucleic Acids Res.* **2016**, *44*, 4539–4550. [[CrossRef](#)]
130. Hsiao, W.; Wan, I.; Jones, S.J.; Brinkman, F.S. IslandPath: Aiding detection of genomic islands in prokaryotes. *Bioinformatics* **2003**, *19*, 418–420. [[CrossRef](#)]
131. Tu, Q.; Ding, D. Detecting pathogenicity islands and anomalous gene clusters by iterative discriminant analysis. *FEMS Microbiol. Lett.* **2003**, *221*, 269–275. [[CrossRef](#)]
132. Rajan, I.; Aravamuthan, S.; Mande, S.S. Identification of compositionally distinct regions in genomes using the centroid method. *Bioinformatics* **2007**, *23*, 2672–2677. [[CrossRef](#)]
133. Bertelli, C.; Laird, M.R.; Williams, K.P.; Group, S.F.U.R.C.; Lau, B.Y.; Hoad, G.; Winsor, G.L.; Brinkman, F.S. IslandViewer 4: Expanded prediction of genomic islands for larger-scale datasets. *Nucleic Acids Res.* **2017**, *45*, W30–W35. [[CrossRef](#)] [[PubMed](#)]
134. Boyd, E.F.; Almagro-Moreno, S.; Parent, M.A. Genomic islands are dynamic, ancient integrative elements in bacterial evolution. *Trends Microbiol.* **2009**, *17*, 47–53. [[CrossRef](#)] [[PubMed](#)]
135. Liu, M.; Li, X.; Xie, Y.; Bi, D.; Sun, J.; Li, J.; Tai, C.; Deng, Z.; Ou, H.-Y. ICEberg 2.0: An updated database of bacterial integrative and conjugative elements. *Nucleic Acids Res* **2019**, *47*, D660–D665. [[CrossRef](#)] [[PubMed](#)]
136. Bi, D.; Xu, Z.; Harrison, E.M.; Tai, C.; Wei, Y.; He, X.; Jia, S.; Deng, Z.; Rajakumar, K.; Ou, H.-Y. ICEberg: A web-based resource for integrative and conjugative elements found in Bacteria. *Nucleic Acids Res.* **2012**, *40*, D621–D626. [[CrossRef](#)]
137. Johansson, M.H.; Bortolaia, V.; Tansirichaiya, S.; Aarestrup, F.M.; Roberts, A.P.; Petersen, T.N. Detection of mobile genetic elements associated with antibiotic resistance in *Salmonella enterica* using a newly developed web tool: MobileElementFinder. *J. Antimicrob. Chemother.* **2021**, *76*, 101–109. [[CrossRef](#)]
138. Campbell, A. Prophage insertion sites. *Res. Microbiol.* **2003**, *154*, 277–282. [[CrossRef](#)]
139. Sousa, A.L.D.; Maués, D.; Lobato, A.; Franco, E.F.; Pinheiro, K.; Araújo, F.; Pantoja, Y.; Costa da Silva, A.L.D.; Morais, J.; Ramos, R.T. PhageWeb—Web interface for rapid identification and characterization of prophages in bacterial genomes. *Front. Genet.* **2018**, *9*, 644. [[CrossRef](#)]
140. Consortium, T.U. UniProt: The universal protein knowledgebase in 2021. *Nucleic Acids Res.* **2020**, *49*, D480–D489.
141. Domsic, J.F.; Avvaru, B.S.; Kim, C.U.; Gruner, S.M.; Agbandje-McKenna, M.; Silverman, D.N.; McKenna, R. Entrapment of carbon dioxide in the active site of carbonic anhydrase II. *J. Biol. Chem.* **2008**, *283*, 30766–30771. [[CrossRef](#)]
142. Le, S.Q.; Gascuel, O. An improved general amino acid replacement matrix. *Mol. Biol. Evol.* **2008**, *25*, 1307–1320. [[CrossRef](#)]
143. Peters, J.E.; Fricker, A.D.; Kapili, B.J.; Petassi, M.T. Heteromeric transposase elements: Generators of genomic islands across diverse bacteria. *Mol. Microbiol.* **2014**, *93*, 1084–1092. [[CrossRef](#)] [[PubMed](#)]
144. Waack, S.; Keller, O.; Asper, R.; Brodag, T.; Damm, C.; Fricke, W.F.; Surovcik, K.; Meinicke, P.; Merkl, R. Score-based prediction of genomic islands in prokaryotic genomes using hidden Markov models. *BMC Bioinform.* **2006**, *7*, 142. [[CrossRef](#)] [[PubMed](#)]
145. Cheng, R.; Li, X.; Jiang, L.; Gong, L.; Geslin, C.; Shao, Z. Virus diversity and interactions with hosts in deep-sea hydrothermal vents. *Microbiome* **2022**, *10*, 235. [[PubMed](#)]
146. Gestal, A.M.; Liew, E.F.; Coleman, N.V. Natural transformation with synthetic gene cassettes: New tools for integron research and biotechnology. *Microbiology* **2011**, *157*, 3349–3360. [[PubMed](#)]
147. Goffredi, S.; Childress, J.; Desaulniers, N.; Lee, R.; Lallier, F.; Hammond, D. Inorganic carbon acquisition by the hydrothermal vent tubeworm *Riftia pachyptila* depends upon high external PCO<sub>2</sub> and upon proton-equivalent ion transport by the worm. *J. Exp. Biol.* **1997**, *200*, 883–896. [[CrossRef](#)] [[PubMed](#)]
148. De Cian, M.C.; Bailly, X.; Morales, J.; Strub, J.M.; Van Dorsselaer, A.; Lallier, F.H. Characterization of carbonic anhydrases from *Riftia pachyptila*, a symbiotic invertebrate from deep-sea hydrothermal vents. *Proteins Struct. Funct. Bioinf.* **2003**, *51*, 327–339. [[CrossRef](#)] [[PubMed](#)]
149. De Cian, M.-C.; Andersen, A.C.; Bailly, X.; Lallier, F.H. Expression and localization of carbonic anhydrase and ATPases in the symbiotic tubeworm *Riftia pachyptila*. *J. Exp. Biol.* **2003**, *206*, 399–409. [[CrossRef](#)]

150. Gonnella, G.; Adam, N.; Perner, M. Horizontal acquisition of hydrogen conversion ability and other habitat adaptations in the *Hydrogenovibrio* strains SP-41 and XCL-2. *BMC Genom.* **2019**, *20*, 339. [[CrossRef](#)]
151. Fabry, V.J.; Seibel, B.A.; Feely, R.A.; Orr, J.C. Impacts of ocean acidification on marine fauna and ecosystem processes. *ICES J. Mar. Sci.* **2008**, *65*, 414–432. [[CrossRef](#)]

**Disclaimer/Publisher's Note:** The statements, opinions and data contained in all publications are solely those of the individual author(s) and contributor(s) and not of MDPI and/or the editor(s). MDPI and/or the editor(s) disclaim responsibility for any injury to people or property resulting from any ideas, methods, instructions or products referred to in the content.